Climate Dynamics

A synoptic decomposition of rainfall over the Cape south coast of South Africa

--Manuscript Draft--

Manuscript Number:	
Full Title:	A synoptic decomposition of rainfall over the Cape south coast of South Africa
Article Type:	Original Article
Keywords:	All-year rainfall region; Cape south coast of South Africa; Synoptic types; Cut-off lows; Ridging high pressure systems
Corresponding Author:	Christien Engelbrecht SOUTH AFRICA
Corresponding Author Secondary Information:	
Corresponding Author's Institution:	
Corresponding Author's Secondary Institution:	
First Author:	Christien Engelbrecht
First Author Secondary Information:	
Order of Authors:	Christien Engelbrecht
	Willem Landman
	Francois Engelbrecht
	Johan Malherbe
Order of Authors Secondary Information:	
Abstract:	A synoptic climatology is derived for the Cape south coast region of South Africa by application of the self-organizing map (SOM) technique. The SOM is applied to average daily low-level circulation fields, as represented by sea-level pressure (SLP) anomalies for the period 1979-2011. This coastal region receives rainfall all-year round with slight peaks during March-April and with more pronounced peaks during August and October-November. The synoptic forcing responsible for this annual multi-modal rainfall distribution is identified, and the relative contribution of different synoptic types to the annual rainfall is quantified. Ridging high-pressure systems contribute to 46% of the annual rainfall, while tropical-temperate troughs contribute 28%. Cut-off lows (COLs) co-occurring with ridging highs and tropical-temperate troughs are associated with 15% of the annual rainfall total. The contribution of ridging high-pressure systems decreases from south to north, whilst the opposite is true for tropical-temperate troughs. COLs, ridging high-pressure systems and tropical-temperate troughs are associated with the March-April rainfall peak, while COLs are largely associated with the August rainfall peak. Ridging high-pressure systems and to a lesser extent tropical-temperate troughs, are responsible for the October peak observed along the coast, while the November peak over the adjacent interior regions is associated with COLs that occur in combination with the tropical-temperate troughs during this month.
Suggested Reviewers:	Alice Favre afavre@csag.uct.ac.za Expert in cut-off lows occurring over South Africa
	Chris Reason chris.reason@uct.ac.za Expert in southern Africa climate variability
	Michael Pook mike.pook@csiro.au Expert in developing synoptic climatology of rainfall; focus on regions in Australian with weather systems similar to that occurring over the Cape south coast of South Africa
	Thando Ndarana thando.ndarana@weathersa.co.za Expert in cut-off lows over southern hemisphere

Authors
Christien J Engelbrecht
1. Agricultural Research Council, Institute for Soil, Climate and Water
2. Department of Geography, Geoinformatics and Meteorology, University of Pretoria
Pretoria
South Africa
engelbrechtc@arc.agric.za
Tel: +2712 310 2676
Fax: +2712 323 1157

Willem A Landman
1. Climate Studies, Modelling and Environmental Health, CSIR Natural Resources and Environment
2. Department of Geography, Geoinformatics and Meteorology, University of Pretoria
Pretoria
South Africa

Francois A Engelbrecht
1. Climate Studies, Modelling and Environmental Health, CSIR Natural Resources and Environment
2. GAES, University of the Witwatersrand, South Africa

Johan Malherbe
Agricultural Research Council, Institute for Soil, Climate and Water
Pretoria
South Africa

Concise title
Synoptic decomposition of rainfall over the Cape south coast of South Africa

Title
A synoptic decomposition of rainfall over the Cape south coast of South Africa

Abstract

A synoptic climatology is derived for the Cape south coast region of South Africa by application of the self-organizing map (SOM) technique. The SOM is applied to average daily low-level circulation fields, as represented by sea-level pressure (SLP) anomalies for the period 1979-2011. This coastal region receives rainfall all-year round with slight peaks during March-April and with more pronounced peaks during August and October-November. The synoptic forcing responsible for this annual multi-modal rainfall distribution is identified, and the relative contribution of different synoptic types to the annual rainfall is quantified. Ridging high-pressure systems contribute to 46% of the annual rainfall, while tropical-temperate troughs contribute 28%. Cut-off lows (COLs) co-occurring with ridging highs and tropical-temperate troughs are associated with 15% of the annual rainfall total. The contribution of ridging high-pressure systems decreases from south to north, whilst the opposite is true for tropical-temperate troughs. COLs, ridging high-pressure systems and tropical-temperate troughs are associated with the March-April rainfall peak, while COLs are largely associated with the August rainfall peak. Ridging high-pressure systems and to a lesser extent tropical-temperate troughs, are responsible for the October peak observed along the coast, while the November peak over the adjacent interior regions is associated with COLs that occur in combination with the tropical-temperate troughs during this month.

1. Introduction

The Cape south coast of South Africa (Fig. 1) receives rainfall all-year round, with peaks during autumn and spring (e.g. Taljaard 1996; Weldon and Reason 2013). The all-year nature of rainfall of this region is in strong contrast to the pronounced seasonality that characterizes rainfall over most of South Africa: the country is largely a summer rainfall region (e.g. Fauchereau et al. 2009), with winter rainfall occurring over the southwestern Cape area (Fig. 1) (e.g. Philippon et al. 2011). The southern areas of South Africa largely receive rainfall from organized synoptic-scale weather systems (Tennant and Hewitson 2002), whilst rainfall over the northern and eastern interior regions are mostly of a convective and sometimes tropical nature (e.g. Malherbe et al. 2012). The all-year rainfall region of the Cape south coast, which to some extent may be thought of as forming a boundary region between the winter and summer rainfall regions, is meteorologically one of the more complex regions of South Africa. Rainfall over the region results from well-defined mid-latitude systems, tropical systems and convection from the north, and complex interactions and linkages between these very different systems. Superimposed on the synoptic circulation there are also meso-scale circulation systems, which result from interactions of the larger scale flow with mountainous topography inland of the coastal area and the moisture laden air above the Agulhas current flowing along the Cape south coast of South Africa. (e.g. Rouault et al. 2002; Singleton and Reason 2006).

Mid-latitude weather systems bringing rainfall to the Cape south coast include cold fronts, west-wind troughs, cut-off lows and ridging high-pressure systems (e.g. Taljaard 1996; Favre et al. 2012; Weldon and Reason 2013). When rainfall over the region is of a tropical nature, it is usually from tropical-temperate trough cloud bands (e.g. Taljaard 1996; Hart et al. 2012). Of the different rain bearing systems, it is mostly COLs that are associated with high-impact events over the region. In fact, across South Africa, COLs are known to on occasion produce 24-hour rainfall totals exceeding the relevant climatological monthly rainfall total at particular locations (e.g. Singleton and Reason 2006; Muller et al. 2008). These systems can be extremely hazardous, producing floods with consequent damage to infrastructure and sometimes loss of life (Weldon and Reason 2013). An important example is the Laingsburg floods of January 1981, in which 104 people drowned in a flood of the Buffels river (Roberts and Alexander 1982; Singleton and Reason 2007b). To date, most rainfall recorded from a single COL event occurred during September 1987 when the 3-day rainfall total along the KwaZulu-Natal coast exceeded 900 mm (Singleton and Reason 2007b). COLs have also been associated with numerous extreme rainfall events along the Cape south coast (e.g. Hayward and van den Berg 1968; Hayward and van den Berg 1970; Rouault et al. 2002; Singleton and Reason 2006; Singleton and Reason 2007a), with the COL event during September 1968 causing floods in the Port Elizabeth area as 500 mm rain fell within 24-hours. These high-impact rainfall events may have led to a perception that COLs are the main rain-producing weather systems over the region.

However, the relative contributions of different weather systems in causing rainfall over the Cape south coast have not been formally quantified. Recently, the contribution of COLs to rainfall over the southern African region has been analysed by Favre et al. (2012). COLs have been shown to explain a higher proportion (more than 20%) of rainfall totals over the Cape south coast compared to the winter and summer rainfall regions (Favre et al., 2012). For this region, the largest contribution of COLs to

rainfall is experienced during the period July to August (JAS), compared to the periods October to December (OND), January to March (JFM) and April to June (AMJ) (Favre et al. 2012). Apart from COLs, ridging high-pressure systems have also been recognised as important in contributing to rainfall over the mountainous regions bordering the Cape south coast (e.g. Weldon and Reason 2013). In fact, it has been suggested that COLs are responsible for the autumn rainfall peak, with ridging high-pressure systems driving the spring rainfall peak over the all-year rainfall region (Jury and Levey 1993). However, the contribution of ridging high-pressure systems to rainfall over the Cape south coast has not been quantified to date. The weather system responsible for the bulk of rainfall over the southern African region is the tropical temperate trough - causing on the average about 39 % of rainfall over the summer rainfall region (Crimp et al., 1997). The maximum frequency of occurrence of tropical-temperate troughs is during November (Hart et al. 2012), when they are also responsible for 30-60% of rainfall occurring along the Cape south coast (Hart et al. 2012). Their relative contribution for December remains high (30-50%) (Hart et al. 2012).

The main aims of this paper are to objectively determine the relative importance of different synoptic types in causing rainfall over the Cape south coast, and to gain more insight into the synoptic climatology that results in the region's all-year rainfall uniqueness. Of particular interest is the relative importance of ridging highs in causing rainfall over the Cape south coast (i.e. compared to COLs). Interactions between ridging highs and COLs, and tropical temperate troughs and COLs in causing rainfall over the region are also considered.

2. Data and methodology

2.1 Weather station data

Rainfall station data for the Cape south coast and adjacent interior extending to the southern escarpment were selected based on completeness (more than 66% of the days in a particular month need to be present and pass data quality tests) of daily rainfall records for the period 1979-2011. Twenty-two weather stations from the South African Weather Service (SAWS) complied with the desired criteria (see Fig. 1 for the locations of the selected stations). The selected station data were subjected to extreme and missing value tests to ascertain data quality. Entries failing these tests were replaced by estimated values derived from neighbouring stations. The beginning of the study period was selected to be 1979, as reanalysis data from the National Centers for Environmental Prediction (NCEP) (Kalnay et al. 1996) prior to 1979 do not have the advantage of satellite data being incorporated into the reanalysis procedure (Tennant 2004). The station data are used in the research to quantify the contribution of different synoptic types to rainfall over the Cape south coast and adjacent interior regions.

Fig. 1 The geographic location of the study region within South Africa (indicated by the rectangle - solid black lines). The 3 sub-regions of interest, labeled as Region 1, Region 2 and Region 3, are delineated by the black dotted lines on the zoomed-in view of the study region. Numbers 1 to 22 indicate the selected rainfall stations used in the analysis of rainfall attributes. The background shaded colour contours of the mean annual rainfall are based on the ARC in-house developed gridded rainfall dataset

2.2 Gridded data

Two independently constructed gridded rainfall datasets, the Femine Early Warning System (FEWS) and the Climatic Research Unit (CRU) version TS3.1, were utilized for the delineation of the all-year rainfall region. Gridded data were used for this purpose rather than the station data described above, due to the uneven distribution in space of stations with records of sufficient length and quality. The FEWS data are a merged satellite-gauge gridded daily rainfall dataset with a resolution of 0.1˚ longitude by 0.1˚ latitude, with records commencing in January 1983 (Sylla et al. 2012). The CRU TS3.1 monthly gridded rainfall dataset has a resolution of 0.5˚ longitude by 0.5˚ latitude, is based solely on station data and is available for the period 1901 to 2009 (Harris et al. 2013). The all-year rainfall region may be defined using the following criteria as guidelines:

- The ratio of the rainfall amount for the month of minimum rainfall to rainfall of the month of maximum rainfall is relatively high compared to regions of strong seasonality.
- Each month of the year needs to be associated with at least 5% of the annual rainfall. This 5% threshold is based on graphs produced by Taljaard (1996), where the monthly contribution to the annual rainfall for various rainfall regions as identified by van Rooy (1972) is presented.

- The average monthly fluctuation of rainfall relative to the average monthly rainfall over the all-year rainfall region should be small compared to that of the winter and summer rainfall regions (see Section 3 for details).

It may be noted that prior to using the gridded datasets for the purpose of identifying the spatial extent of the all-year rainfall region, it was first established that these rainfall sets sufficiently describe the intra-annual rainfall cycle over South Africa. This was achieved through a comparison of the monthly rainfall climatologies of the gridded datasets against those of the selected whether stations, as well as those of a third gridded rainfall climatology. The latter was developed at the Agricultural Research Council (ARC), using station data from both the ARC and SAWS. Despite the general underestimation of rainfall totals over Africa in FEWS data, in particular over regions of orography (Sylla et al. 2012), both datasets have been found to give representations of the area of all-year rainfall consistent with the raw weather station data and the mentioned ARC dataset. The mean annual distribution of rainfall over South Africa, as described by the ARC dataset, is shown in Figure 1. Note that mean annual rainfall totals exceeding 1000 mm occur in places along the Cape south coast.

2.3 Atmospheric circulation data

Daily averaged sea-level pressure (SLP) and geopotential height data from NCEP reanalysis data, NCEP 1 (Kalnay et al. 1996), for the period January 1979 to December 2011 are utilized. The NCEP data has a horizontal resolution of 2.5˚ by 2.5˚ and a vertical resolution of 17 pressure levels. The daily weather over the Cape south coast region is strongly dependent on the low-level circulation, and the main source of moisture is the ocean. In particular, major rainfall events over the region are associated with the low-level moisture flux originating from the Agulhas current to the southeast (e.g. Rouault et al. 2002; Singleton and Reason 2006; Singleton and Reason 2007a). Therefore, daily SLP is employed for the identification of low-level circulation patterns.

2.4 Weather pattern identification

Weather patterns that influence the Cape south coast region of South Africa were objectively identified by application of the self-organizing map (SOM) technique (Kohonen 2001). The technique is based on an unsupervised nonlinear clustering algorithm that organizes the input data into a user-specified number of nodes that span the continuum of types in the input data. The technique is well suited for weather pattern identification where the daily transitions between weather patterns are important (Hewitson and Crane 2002). SOMs are increasingly being employed in climate studies focusing on the southern African region (e.g. Hewitson and Crane 2002; Tennant and Hewitson 2002; Tozuka et al. 2013; Van Schalkwyk and Dyson 2013). NCEP reanalysis daily averaged SLP data for the period 1979-2011 was used to develop a SOM relevant to the Cape south coast region. Daily SLP anomalies at each grid point were calculated by subtracting the daily domain-averaged SLP from the SLP at each grid point. This procedure effectively eliminates seasonal rises and falls in the geopotential from influencing the nodes identified by the SOM. Through the use of anomalies as specified above, the daily weather patterns are effectively used in the construction of the SOM. A similar approach was followed by Schuenemann et al. (2009). The SOM was constructed for the region 45º S to 32.5º S and 10º E to 40º E. The selected region allows for capturing the progression of high pressure systems and troughs, advancing from west to east, to the south of the Cape south coast. The northern boundary of the SOM region was purposefully selected to extend to only 32.5º S. If this boundary is chosen further to the north, to include most of the interior of South Africa, the synoptic types identified by the SOM are dominated by the prevailing wintertime high pressure systems over the interior. Furthermore, SLP is used as a variable to develop the SOM, as the circulation over the oceans bordering the subcontinent is crucial in inducing rainfall over the Cape south coast (see Section 2.3). It may be noted that tropical-temperate trough linkages are captured with the SOM configuration as described, even though the northern boundary of the SOM region is limited to the extreme southern parts of the interior (see Section 3). The typical SLP patterns associated with COLs (e.g. Taljaard 1985; Tennant and van Heerden 1994) are also captured. For the purpose of this study, it is appropriate to apply a relatively large SOM to avoid over generalizing the richness of weather patterns that occur over the region into a too small number of nodes (synoptic types). SOMs that classify daily SLP circulation into 12, 20 and 35 synoptic types, respectively, have been considered. It was found that the 12 and 20 node SOMs do not capture the various stages of sea-level anticyclones, ridges and troughs adequately. Of particular importance, is that the known variations in the position and amplitude of SLP ridges and troughs that are representative of weather patterns ranging from weak synoptic flow to tropical-temperate troughs and COLs, are well represented in the SOM.

Following Schuenemann et al. (2009), the statistical significance of the frequency for which the daily SLP anomalies map to each node is determined by calculating a 95% confidence interval around the probability that any daily SLP anomaly would map to any node (2.86% for the 7x5 SOM used in this study). By assuming that the process is binomial, the 95% confidence limits are calculated by

$$p \pm 1.96 \left[\frac{p(1-p)}{n}\right]^{1/2},$$

where p is 2.86% (the probability that any daily SLP anomaly field would map to any node) and n is 12053 (number of daily SLP anomaly fields). The calculated confidence interval around 2.86% is 2.56 to 3.15%. The observed frequency of a node is considered significantly different from 2.86% at the 95% confidence level if it falls outside this calculated interval.

2.5 Identification of cut-off lows

On the average, only about 11 COLs occur annually over the southern African region (Singleton and Reason 2007b), implying that these systems would not feature as a stand-alone synoptic type in the 7x5 SOM based on daily circulation fields presented in this paper. Indeed, COLs may occur in conjunction with a number of different low-level circulation patterns - most commonly in association with a strong ridge of high pressure in the low-levels polewards of the upper COL (e.g. Taljaard 1985; Tennant and van Heerden 1994; Katzfey and McInnes 1996), in combination with tropical-temperate troughs (Hart et al. 2012), and further, as a COL system evolves, in association with the evolving high pressure system (ridging progressively from the southwest to southeast of South Africa). An objective tracking methodology is therefore used in order to study the effects of these important rainfall producing systems on rainfall attributes over the Cape south coast region.

NCEP reanalysis data (Kalnay et al. 1996) was utilized for the purpose of identifying and tracking COLs over the period 1979-2011. Over South Africa, COLs exhibit a typical length scale of 1000 km (e.g. Singleton and Reason 2007b) and are therefore well resolved on the 2.5˚ resolution grid of the NCEP data. In this paper, a COL is defined as a closed-low (a local minimum in the geopotential height at the 500 hPa level) that possesses a cold core, following the criteria used by Favre et al. (2012). The daily-average geopotential height and temperature fields at 500 hPa are utilized for identifying and tracking COLs. It was decided to select for the analysis only well-established COLs, with a life span of at least two days - effectively filtering out cases of short-lived closed-low formation. The closed-lows are identified and tracked by applying an objective, automated tracking algorithm (Engelbrecht et al. 2013). Geopotential minima are identified by comparing the geopotential of each grid point in the domain bounded by 40˚ S – 20˚ S and 10˚ E – 40˚ E, to the geopotential values of the square of eight surrounding grid points on the latitude longitude grid. Closed-low tracks are constructed by identifying the geopotential minima of time step *t+1* nearest to the geopotential minima at time step *t*, provided that this distance is less than 1000 km. This distance implies that closed-lows are assumed not to move faster than 42 km/h (Favre et al. 2012). The tracking procedure is developed in such a manner that any geopotential minima can only be part of a single track (see Engelbrecht et al., 2013 for details). All the closed-lows identified through the procedure outlined above are subsequently subjected to a cold-core test. The approach utilized by Favre et al. (2012) is applied in this study. For each of the closed-lows, a temperature minimum needs to be located within 600 km of the geopotential height minimum, in order for the low to be defined as a cold-core low. To accommodate hybrid systems (systems that also display some partial barotropic/warm core characteristics during their life time), the old-core requirement is somewhat relaxed – it is required for a cold-core to be present for only half of the time-steps (or more), for a track to be classified as a COL track. An important difference between the analysis performed here and those of Engelbrecht et al. (2013) and Favre et al. (2012), is the focus on well-established, long life-span COLs. The former study considered closed-lows in general, with no cold-core requirement, and the systems were required to have a life span of at least one day (rather than two days as in this study). In the case of Favre et al. (2012) all closed-low cold-core occurrences were considered, irrespective of the life-spans of the systems. Systems were also required to exhibit cold-core characteristics for only a single time-step during the life-span of a system, rather than for at least half of the time-steps for systems with a life span of at least two days as in the analysis represented here.

Rainfall associated with cold-cored systems occurs mainly some hundreds of kilometers to the northeast, east and southeast of the centers of these systems (Taljaard 1995). From the constructed

COL dataset for the period 1979-2011, all the COLs that occurred within 1100 km from the centroid of the study region (see Fig. 1) were considered to be potentially responsible for rainfall over the region. Such COLs associated with rainfall over the study region, at least at a single station, are defined as rainfall producing COLs. Finally, for each day that a COL was identified as rainfall-producing over the study area, the circulation of that day was mapped onto the synoptic types identified by the SOM. This enables the identification of the synoptic types that are most frequently associated with COLs that influence the study area.

2.6 Relating rainfall to the identified synoptic types

To relate rainfall to the main synoptic types identified by the SOM, daily rainfall data (1979-2011) for weather stations in the Cape south coast region and adjacent interior were mapped to the SOM. That is, for each day in the time-series the relevant circulation pattern may be associated with one of the SOM's synoptic types (e.g. Tennant 2003). The corresponding daily rainfall totals are subsequently associated with the relevant synoptic type, on a station-by-station basis. This enables calculating the percentage of annual rainfall associated with a specific synoptic type for each station in the region. Note that the study region allows for the contributions of different synoptic types to rainfall over the all-year rainfall region to be compared to contributions to rainfall over the summer rainfall region to the north (Fig. 1). The spatial distribution of rainfall over the study region exhibits a marked north-south gradient, with annual rainfall totals exceeding 1000 mm along the Cape Folded mountain range in the south whilst less than 200 mm of rain is observed over the Karoo just north of the Cape Folded mountain range. Further to the east, over the interior of the study region, the annual rainfall totals vary between 300 and 700 mm. These different rainfall distributions were used to identify 3 separate regions for which rainfall was categorized according to the different synoptic types (see Section 3 for details). The percentage contribution by each node to the annual rainfall for a particular region was calculated by averaging the percentage contributions to rainfall recorded at each of the weather stations in the particular region.

3. Results

3.1 Attributes of rainfall over the Cape south coast and adjacent regions

3.1.1 Spatial extent of the all-year rainfall region

Application of the criteria describing all-year rainfall attributes (see Section 2.2) on CRU TS3.1 and FEWS mean monthly rainfall data, yields remarkably similar spatial patterns (Fig. 2) – across the 3 different metrics, and across the 2 data sets. Qualitatively, the metrics indicate that the spatial extent of the area receiving rainfall all-year round along the Cape south coast is found within the collective boundaries described in other studies (e.g. Taljaard 1996; Landman et al. 2001; Rouault and Richard 2003; Weldon and Reason 2013). Along the coast, the all-year rainfall region is found approximately between 21º E and 27º E, while its northern extent is mostly restricted by the Cape Folded mountain range (not shown – about 33.7 °S). The extent of the all-year rainfall region is well illustrated by the metric of the number of months of the year that receive 5% or more of the annual rainfall. In both CRU (Fig. 2c) and FEWS (Fig. 2d), 11-12 months of the year satisfies the criteria over the mentioned area. Weather stations number 1 to 12 in Figure 1 are located in this region – and all receive 5% or more of the annual rainfall total during each month of the year. This region will be referred to as Region 1 in the study and from here onwards is regarded to define the Cape south coast (or all-year rainfall) region. The data from weather stations number 1 to 12 as seen on Figure 1 are used for the analysis concerning rainfall attributes of Region 1. From the western part of the all-year rainfall region along the Cape south coast, a relatively narrow region that exhibits pseudo all-year rainfall characteristics extends northwards, to the east of the western escarpment (see the arrows in Figs. 2c and 2d). As the main focus of this study is on the Cape south coast, this secondary all-year rainfall region is analysed separately as Region 2. It is defined to have 32.3 °S as northern boundary and 22.8 °E as eastern boundary, and includes weather stations number 13 and 14 (Fig. 1). For these two stations all months, with the exception of September, receive 5% or more of the annual rainfall. Region 3 comprises of weather stations number 15 to 22. Region 3 exhibits summer rainfall characteristics, as seen in the ratio of the month of minimum rainfall to the month of maximum rainfall (Fig. 2a, b). For the stations located in this region, at least 3 months receive on the average monthly rainfall totals that are less than 5% of the annual rainfall. It may finally be noted that there is a small area along the north coast of KwaZulu-Natal that also exhibits all-year rainfall attributes, according to the metrics presented in Figure 2. The circulation dynamics of this region are likely to be very different to that of the Cape south coast, and its investigation falls beyond the scope of the current paper.

Fig. 2 Delineation of rainfall regions in South Africa according to the ratio of the month of minimum rainfall to the month of maximum rainfall (a, b), the number of months for which the mean monthly rainfall total contributes 5% or more to the mean annual rainfall total (c, d), and the average fluctuation of monthly rainfall from the monthly main rainfall expressed as a percentage (e, f), calculated from CRU (a, c, e) and FEWS (b, d, f) data for the period 1983-2009

3.1.2 Annual rainfall cycle

The annual rainfall cycle over Region 1 (based on the monthly rainfall totals averaged over weather stations number 1 to 12) exhibits 3 peaks (Fig. 3). These peaks occur during March-April, August and October, with the October peak of 80 mm being the highest (monthly totals averaged over the period 1979-2011 are shown). A rainfall hiatus occurs in September. Region 2 has rainfall peaks during April and November (based on weather stations number 13 and 14), with April the month with the highest rainfall total. Over Region 3, a summer rainfall region, rainfall peaks over the period November to March. The November peak is slightly higher than the February-March peak. The September rainfall hiatus is present over Regions 2 (Fig. 3b) and 3 (Fig. 3c) as well, although less prominent in amplitude compared to the Region 1 hiatus. (Fig.3a). A key objective of the paper is to explain the existence of the three rainfall peaks of Region 1, from a synoptic type perspective.

Fig. 3 Area-averaged annual rainfall cycle for the period 1979-2011 over (a) Region 1, (b) Region 2 and (c) Region 3 as described by weather station data (solid line) and FEWS rainfall (dotted line)

Regarding the delineation of the all-year rainfall region, the application of the all-year rainfall criteria on CRU and FEWS rainfall data produced in general similar results and is useful to describe the spatial extent of the region (Fig. 2). Application of the criteria to the weather station data produced consistent results. Similarly, the annual rainfall cycle described by the weather station data for Regions 1 to 3 is qualitatively captured by the FEWS rainfall estimates (Fig. 3) and CRU data (not shown). That is, despite the monthly rainfall totals being underestimated by FEWS, the annual rainfall cycle with respect to the peaks and September hiatus is captured. All subsequent rainfall analyses presented in this study are based on the weather station data.

3.2 Synoptic type classification

Figure 4 shows the synoptic type classification produced by the SOM algorithm. Each node in the SOM represents a single SLP anomaly pattern representative of a portion of the 12053 daily patterns used to train the SOM. The frequency of occurrence for each of the nodes is indicated at the top right of the relevant node, with the node number shown at the top left (Fig. 4).

Fig. 4 SOM of SLP anomalies (hPa) based on daily NCEP reanalysis data from 1979 to 2011. Anomaly SLP contour interval is 2 hPa. Blue and red shades represent negative and positive SLP anomalies, respectively. The node numbers as well as the node frequency of occurrence are indicated on the figure. Nodes occurring outside the range of 2.56-3.15%, have lower or higher than average occurrences statistical significant at the 95% confidence level. Subjective clustering of the main synoptic types is indicated and represent ridging high pressure systems southeast of the subcontinent (RE), tropical-temperate troughs (TTT), troughs southwest of the subcontinent (TSW), troughs southeast of the subcontinent (TSE), ridging high pressure systems from the southwest (RSW) and weak synoptic flow (WSF)

Fig. 5 Sammon map for the SOM shown in Fig. 4

On a SOM, similar synoptic patterns are grouped together with nodes characterized by very different patterns being further apart. From the Sammon map shown in Figure 5 it can be seen that the nodes in the top half of the SOM, in particular the top-middle region, are more similar to adjacent nodes compared to the nodes found in the lower half of the SOM. Generally, the lower part of the SOM is occupied by circulation patterns typical of winter, the upper part by circulation patterns typical of summer and the central part by circulation patterns occurring throughout the year. The nodes that occur most frequently during each month of the year may be discerned from analysis presented in Figure 6. The circulation patterns represented in the lower left corner of the SOM (Fig. 4) are strong frontal troughs that occur most frequently during June to August (Fig. 6g, h, i). For September (Fig. 6j), the nodes occurring most frequently are placed in the lower right corner of the SOM. Here, the paths of the

391 frontal troughs are displaced slightly polewards compared to the winter tracks, allowing for the
392 Atlantic Ocean High (AOH) to extend a ridge along the southern coastal belt of the subcontinent,
393 mainly overland. At the start of the summer season (Fig. 6k, l) and during December (Fig. 6a), ridging
394 high pressure systems from the southwest ridge from further south (nodes middle and upper right part
395 of the SOM) as the frontal troughs continue to be displaced polewards, with a cell of high pressure
396 moving eastwards to be situated southeast of the subcontinent (upper left corner of the SOM). For
397 January, February and March (Fig. 6b, c, d), the nodes in the upper part of the SOM represent the
398 dominant synoptic types. These nodes are representative of the various configurations of tropical-
399 temperate troughs, transforming to tropical-temperature linkages over the western interior during April
400 (Fig. 4 node 15, Fig. 6e). By May (Fig. 6f), the nodes representative of frontal troughs that have
401 migrated equatorward after the summer months, are becoming more frequent again.
402
403 **Fig. 6** Node frequencies (%) for (a) December (1023 days), (b) January (1023 days), (c) February (932
404 days), (d) March (1023 days), (e) April (990 days), (f) May (1023 days), (g) June (990 days), (h) July
405 (1023 days), (i) August (1023 days), (j) September (990 days), (k) October (1023 days) and (l)
406 November (990 days) that map to each node based on the total days of the particular month from 1979-
407 2011
408
409 **3.3 Relative contribution of synoptic types to rainfall over sub-regions**
410
411 The regionally-averaged daily rainfall associated with each node as well as the percentage contribution
412 of each node to the annual rainfall over each of the regions are shown in Fig. 7. The COLs identified by
413 the tracking algorithm were mapped to the relevant node of the SOM for inclusion in the analysis with
414 regards to the relative contribution of the synoptic types to the annual rainfall over the sub-regions
415 (Fig. 8). During 1979-2011, 190 COL events (361 COL days) were associated with rainfall over the
416 study region. COL-induced rainfall over the study region is mostly associated with COLs located over
417 the southwestern interior (Fig. 8).
418
419 Over all the regions, nodes in the upper right part of the SOM are responsible for a relatively large
420 contribution to the annual rainfall (Fig. 7d, e and f). These nodes are typical of the late summer months,
421 February and March (Fig. 6). Over the Cape south coast (Region 1), the six nodes in the upper right
422 corner are responsible for 43% of the annual rainfall (Fig. 7d), while the frequency of occurrence of
423 these nodes is only 17% (Fig. 4). These nodes represent the AOH that extends a ridge eastwards at
424 about 40˚ S (nodes 27, 28, 35), as well as tropical-temperate troughs (nodes 26, 33, 34). Node 35 is
425 associated with the largest average daily rainfall over Region 1 (Fig. 7a) and Region 3 (Fig. 7c). It also
426 has a significantly higher than average occurrence, which in combination with the high average daily
427 rainfall totals lead to this node being associated with 13% and 11% of the annual rainfall over Regions
428 1 (Fig. 7d) and 3 (Fig. 7f), respectively. It may further be noted that this node is associated with the
429 highest frequency of COLs associated with rainfall over the region (Fig. 8). Node 14 is also associated
430 with high average daily rainfall totals over Region 1 (Fig. 4). This node has a maximum frequency of
431 occurrence during winter (Fig. 6), and represents a high pressure system ridging behind a frontal
432 system that is situated southeast of the subcontinent.
433
434 Nodes 15, 22 and 29 (Fig. 4) are prominent in contributing to the annual rainfall over Regions 2 and 3.
435 Nodes 15 and 22 represent tropical-temperate linkages. Node 29 is characterized by a high pressure
436 system southeast and south of the subcontinent, and of all the nodes is associated with the second
437 highest frequency of COLs (Fig. 8). The association of node 29 with COLs as well as the location of
438 the surface trough in the extreme west are probably the reasons for this node being responsible for the
439 highest average daily rainfall over Region 2 (Fig. 7b). The higher than average occurrence of node 29
440 is statistically significant at the 95% confidence level. It contributes 16% of the annual rainfall
441 occurring over Region 2 (Fig. 7e). The nodes representative of frontal troughs located in the lower and
442 middle central part of the SOM, are generally associated with small average daily rainfall totals over all
443 the regions, and consequently with the smallest contribution to the annual rainfall.
444
445 **Fig. 7** The regionally averaged daily precipitation (mm/day) for each SOM node for (a) Region 1, (b)
446 Region 2 and (c) Region 3, and the average annual contribution (%) by node to rainfall over (d) Region
447 1, (e) Region 2 and (f) Region 3
448
449 **Fig. 8** Accumulated frequency of rainfall-producing COLs (units: COL days/grid point) for each SOM
450 node for the period 1979-2011. Only grid points with a frequency of at least 1 day are indicated

The 35 synoptic types may be subjectively grouped into main synoptic classes that are relevant to the Cape south coast region. These are troughs southwest and southeast of the subcontinent, ridging high pressure systems from the southwest, high pressure systems located east of the subcontinent, tropical-temperate troughs and weak synoptic flow (Fig. 4). The clustering of the 35 nodes into the 6 main synoptic classes is based on additional evaluation of composite maps of the 850, 700, 500, 200 hPa geopotential heights as well as the spatial distribution of rainfall over southern Africa associated with each node (not shown). The spatial rainfall distribution over southern Africa is employed to aid in the identification of nodes representative of tropical-temperate troughs – characterized by the presence of a cloud band originating from tropical Africa extending south or southeastwards over South Africa (e.g. Hart et al. 2012). As the station data used is limited to the study region, the FEWS rainfall estimate was employed to represent the spatial rainfall distribution associated with each node over southern Africa.

Fig. 9 The percentage contribution to the average annual rainfall of the 6 main synoptic classes identified in this study for (a) Region 1, (b) Region 2 and (c) Region 3. The percentage of rainfall contributed by COLs to the average rainfall, in association with the six main synoptic classes, is shown in yellow

Of the six synoptic classes identified, high pressure systems ridging from the southwest contribute most to rainfall over Region 1 (Fig. 9a, bar 3). In fact, the various configurations of these systems are associated with a staggering 46% of the region's rainfall. The subset of ridging highs from the southwest occurring in conjunction with COLs contributes 6% to total annual rainfall. It is likely though, that the remaining cases are often associated with other forms of upper-air support (e.g. upper air troughs). Still, this result is indicative that the low-level flow around favorably positioned near-surface highs, and possible interactions with the mountainous topography adjacent to the coastal area, are factors of key importance in causing rainfall over the Cape south coast region. Over Regions 2 and 3 (Fig. 9b, c, bar 3), the contribution of ridging high-pressure systems from the southwest to the annual rainfall is much less – 22 and 30% respectively (7% and 5% in conjunction with COLs respectively). This result confirms that it is the low-level flow and interaction with topography that causes this synoptic class to be of key importance to the Cape south coast region itself. Tropical-temperate troughs contribute to 28, 38 and 37% of the annual rainfall over Regions 1, 2 and 3 respectively (Fig. 9a, b, c, bar 5). The overall contribution of COLs to the annual rainfall over the Cape south coast is 15%, much less than the contribution of 40% of ridging highs that occur in the absence of COLs. Favre et al. (2012) have found the contribution of COLs to annual rainfall over the Cape south coast to be somewhat higher – in the order of 20 to 30%. However, they considered all cases of closed-low occurrences and less strict criteria for the presence of cold-cores in their analysis. COLs are estimated to contribute about 22% and 14% of the annual rainfall over Region 2 and 3 respectively. Taking into account that only a small number (6 on the average) of COLs contribute to rainfall over the Cape south coast per year, the relatively large portion of rain these systems contribute to the annual rainfall is quite noteworthy. Not surprisingly, when extreme daily rainfall are considered, defined here as the 95th percentile of all recorded days with rainfall at one station or more over a particular region, the contribution of COLs to extreme rainfall events is 36, 52 and 38%, over Regions 1, 2 and 3 respectively.

3.4 Synoptic types driving the annual rainfall cycle over the Cape south coast

The decomposition of the synoptic types responsible for rainfall over the Cape south coast performed in the previous section shows the relative importance of ridging high pressure systems, tropical-temperate troughs and COLs over this region. The role that each of these systems play in the annual rainfall cycle over the region will subsequently be discussed. Of particular interest is the role of COLs and their association with the observed rainfall peaks (Fig. 2), since COL occurrences over South Africa reach maximum numbers during March-May and October (Singleton and Reason 2007b; Favre et al. 2012), corresponding with two of the three rainfall peaks observed over the all-year rainfall region of South Africa. Moreover, COLs are associated with significant rainfall events along the Cape south coast region (e.g. Taljaard 1985; Singleton and Reason 2006; Singleton and Reason 2007a, also see Section 3.3). In order to investigate the relative contribution of COLs to the rainfall cycle over the Cape south coast, the percentage contribution of COLs to monthly rainfall totals was calculated.

Over the 33-year period analysed, 190 rain-producing COLs occurred within 1100 km from the centroid of the study region. The preferred geographical location of these COLs is the southwestern interior of South Africa and adjacent oceanic area off the west coast (Fig. 8). This region has been

identified by Favre et al. (2012) and Engelbrecht et al. (2013) as being one of the areas of southern Africa with the highest frequency of COLs. Winter (June-August) and spring (September-November) have the highest frequency of occurrence of COLs over the study region, with frequencies particularly high in June, August and November (Fig. 10). Interesting to note is that November is also the month with the highest occurrence of tropical-temperature troughs over southern Africa (Hart et al. 2012). Over the study region, August and November seem to be the important months with regard to COL-induced rainfall. On a quarter of all COL associated rain days during these months, rainfall that is reported at more than 60% of the weather stations over the study region.

Fig. 10 Accumulated monthly number of COLs within 1100 km from the centroid of the study region and associated with rainfall at 1 station or more, over the period 1979-2011

Synoptic types associated with the March-April rainfall peak over Region 1 (Fig. 11a) include troughs, ridging high pressure systems and tropical-temperate troughs, with nodes 21, 28, 33, 34, 35 being the most prominent in contributing rainfall during March, and nodes 7, 14, 21, 26, 28, 33, 34, 35 the most prominent during April (Fig. 12a). Ridging high pressure systems and tropical-temperate troughs accompanied by COLs contribute significantly to this rainfall peak while these systems in the absence of COLs contribute to a lesser extent to the rainfall peak (Fig. 11a). During March, COLs occur in combination with ridging high pressure systems from the southwest and tropical temperate troughs (represented by nodes 26, 34 and 35). The rainfall peak during April associated with COLs is characterized by accompanying ridging high pressure systems from the southwest and- southeast as well as tropical temperate troughs – nodes 21, 22, 29, 34 and 35 are representative of the aforementioned synoptic types (Fig. 12d). Over Region 2, the March-April peak (Fig. 11b) in rainfall is associated with troughs from the southwest, ridging high pressure systems and tropical-temperate troughs. Nodes 9, 15, 22, 29, 34 and 35 are representative of the synoptic types contributing the most to the rainfall peak during March while nodes 14, 15, 16, 17, 22, 28, 29, 33, 34 and 35 are prominent during April (Fig. 12b). The synoptic types associated with COL-induced rainfall that contribute most prominently to the rainfall peak during March are representative of nodes 22, 26, 29, 31, 34 and 35 (Fig. 12e). During April, the rainfall peak is clearly driven by COL-induced rain. Nodes 29 and 35 are representative of the synoptic types that accompany COLs during April, with node 29 in particular prominent to contribute to the rainfall peak (Fig. 12e). Over Region 3, January to March experience the same rainfall-producing synoptic types (node 8, 9, 15, 16, 22, 29, 33), with the rainfall peak occurring in February, driven by tropical-temperate troughs as represented by nodes 15, 22, 29 and 33 (Fig. 12c).

During August, COLs associated with nodes 29 and 35 (Fig. 12d) as well as ridging high pressure systems (nodes 21, 28, 35) and tropical-temperate troughs (nodes 26, 34) contribute to the rainfall peak over Region 1 (Fig. 12a and 11a). Over Regions 2 and 3, the August rainfall peak is significantly less prominent than the autumn and spring peaks. For Region 2, the analysis reveals that COL-induced rainfall is mainly responsible for the small-amplitude August peak in the annual rainfall cycle (Fig. 11b). During this time COLs occur in association with nodes 22 (tropical temperate troughs) and 29 (ridging high-pressure systems southeast of the subcontinent). A small amplitude August rainfall peak is also present over Region 3 (Fig. 11c) and seems to occur in association with synoptic types 13, 14, 28, 31, 34 and 35. The analysis in this case is not indicative of a link to COLs.

The month of October is characterized by a prominent rainfall peak over the Cape south coast, and strong rises in the monthly rainfall totals compared to the September totals over all three regions (Fig. 11). However, Figure 11 also reveals that COL-induced rainfall doesn't peak or rise significantly relative to September totals during October. Ridging high pressure systems from the southwest (nodes 14, 20, 28, 35), tropical-temperate troughs (nodes 33, 34) and high pressure systems southeast of the subcontinent (node 29) are associated with the October rainfall peak over Region 1 (Fig. 12a). Of these weather systems, ridging high pressure systems from the southwest are responsible for the largest contribution to the rainfall peak. Over Regions 2 and 3 ridging high pressure systems from the southwest, a ridge southeast of the subcontinent and tropical-temperate troughs (nodes 15, 28, 29, 30, 34, 35 and nodes 15, 28, 29, 33, 34, 35 respectively) are the main synoptic types contributing to the October rainfall (Fig. 12b, c). The largest contribution to the October rainfall over Region 2 is from a ridge southeast of the subcontinent, represented by node 29 (Fig. 12b) while tropical-temperate troughs contribute most to October rainfall over Region 3 (Fig. 12c). November is the month with the highest frequency of rain-producing COLs (Fig. 10) as well as tropical-temperate troughs (Hart et al. 2012). The November rainfall peaks over Region 2 (Fig. 11b) and Region 3 (Fig. 11c) can be ascribed to

570 COLs (Fig. 11e, f) and their interaction with tropical-temperate troughs. COLs also contribute to the
571 relatively high rainfall totals over Region 1 in November (Fig. 11a).
572
573 **Fig. 11** Area-average annual rainfall distribution for the period 1979-2011 over (a) Region 1, (b)
574 Region 2 and (c) Region 3. The black solid line represents the monthly rainfall (%), the black dotted
575 line the monthly rainfall associated with COLs (%) and the red dotted line the monthly rainfall without
576 the COL-induced rainfall (%)

577 **Fig. 12** Percentage contributions of monthly rainfall totals to the average annual rainfall (y-axis) not
578 associated with COLs for (a) Region 1, (b) Region 2, (c) Region 3 and associated with COLs for (d)
579 Region 1, (e) Region 2 and (f) Region 3. The 35 SOM nodes are indicated on the x-axis
580
581 **4. Discussion and Conclusions**

582 The Cape south coast of South Africa, here defined as the region between 21 and 27 °E and south of
583 the Cape folded mountains (that is, south of about 33.7 °S), is an all-year rainfall region. Over this
584 region, at least 11 but mostly all 12 months of the year contribute 5 % or more to the long-term average
585 annual rainfall total, in both gridded (CRU TS3.1 and FEWS) and weather station data analysed over
586 the region. Other features that distinguish the region from the winter and summer rainfall regions of
587 South Africa is the relatively high ratio of the rainfall total for the month of minimum rainfall to the
588 total for the month of maximum rainfall, and the relatively small average fluctuation of monthly
589 rainfall totals around the monthly mean rainfall total.

590 The SOM technique was used to develop a synoptic climatology for the Cape south coast of South
591 Africa, and the synoptic forcing of rainfall over the region was subsequently analysed. NCEP
592 reanalysis daily SLP anomaly data were used to train a 7x5 SOM. A number of well-known synoptic
593 classes, such as ridging highs, tropical-temperate troughs and weak synoptic flow have been identified
594 by the SOM, as well as subtle but systematic differences within different synoptic types that make up
595 the main classes. The importance of the SOM to capture these subtle differences is illustrated by the
596 nodes' very different contributions to annual rainfall over the region. This is applicable in particular to
597 the rain-producing synoptic types, such as ridging high pressure systems from the southwest and
598 tropical-temperate troughs. For example, the results presented in this paper indicate that ridging high-
599 pressure systems where the ridge is located further southwards are more conducive to rainfall along the
600 Cape south coast region than ridges located more equatorwards, even if the pressure distribution is
601 otherwise similar. A similar observation was made regarding the intensity of the ridging high pressure
602 systems. It has long been known that the geographical location and the intensity of ridging high
603 pressure systems is a determining factor for the occurrence of rainfall and the nature of the rainfall over
604 the Cape south coast region (e.g. Taljaard 1996). However, by application of a SOM, it is possible to
605 quantify the rainfall associated with the different types within a main synoptic class. For example, over
606 the 33-year period node 27 (ridging high pressure system from the southwest) yielded 3.6 mm/day,
607 whereas node 28 (also a ridging high- pressure system from the southwest) yielded 5.8 mm/day.
608 Similarly, ridging high pressure systems from the southwest represented by nodes 20 and 21 yielded
609 approximately 1.6 and 3.6 mm/day. Taking the frequency of occurrence of the synoptic types into
610 account, the contribution by a single type within a main synoptic class (e.g. ridging highs) becomes
611 important with regard to seasonal or annual rainfall totals.

612 Ridging high pressure systems are the synoptic types that contribute most to rainfall totals over the
613 Cape south coast region. These systems have a frequency of occurrence of 23% (of the total number of
614 daily occurrences of synoptic types) but contribute 46% of the total rainfall over the Cape south coast.
615 Over Regions 2 and 3, the contribution of ridging high pressure systems to rainfall totals is notably
616 less, which suggests that topography plays some part in enhancing the rainfall along the coast (Region
617 1). Tropical-temperate troughs are responsible for 28% of the rainfall over Region 1, increasing
618 northwards to contribute 38% and 37% to the annual rainfall over Regions 2 and 3. The frequency of
619 occurrence of the various configurations of tropical-temperate troughs accumulates to 25%. COLs
620 occur in combination with ridging high pressure systems (ridging from the southwest and southeast)
621 and tropical-temperate troughs. However, the contribution to rainfall by COLs has been isolated from
622 these systems for comparison purposes using an objective tracking algorithm. COLs contribute 15%
623 (6% in co-occurrence with ridging highs), 22% and 14% to the annual rainfall over Regions 1, 2 and 3
624 respectively. The contribution to rainfall by COLs is remarkable, considering that the COL-induced
625 rainfall days over the Cape south coast region amount only to 2.4%. Transient frontal troughs were
626 found to bring the least rain to Region 1 of the rain-bearing systems, consistent with the observations of

the winter months being associated with a season characterized by lower rainfall totals compared to transitional seasons.

The autumn and August rainfall peaks observed in the annual rainfall cycle over the Cape south coast (Region 1) cannot be attributed to a single rain-producing synoptic type. Both ridging highs and COLs have been shown to contribute to these rainfall peaks, but with COLs being more dominant during August. In fact, over the interior (Region 2 and 3) COLs are the single synoptic type driving the August rainfall peak, as rainfall associated with ridging high pressure systems is limited to the seaward side of the Cape folded mountain range. The September hiatus in rainfall that occurs across the three regions, after the August peak, seems to be related to a poleward displacement of frontal systems and positioning of high-pressure systems (ridging mainly over land) that are both unfavorable for rainfall. Along the Cape south coast, the October rainfall peak is the highest rainfall peak observed during the year. This rainfall peak is the result of ridging high pressure systems and to a lesser extent tropical-temperate troughs, with an insignificant contribution by COLs. The increase in rainfall during October is also observed over the interior regions. However, the rainfall peak over Regions 2 and 3 occurs in November when an increase in COL-induced rainfall is observed over all the regions. This November peak can largely be attributed to COLs. Noteworthy is the importance of ridging high pressure systems relative to COLs for the existence of the October rainfall peak along the coast (Region 1).

Acknowledgements

This research was funded by the Water Research Commission (Project K5/2257/1) and the Applied Centre for Climate and Earth System Studies (ACCESS) in South Africa. The editing contributions of Dr Fyfield from the Agricultural Research Council are acknowledged.

References

Crimp SJ, van den Heever SC, D'Abreton PC, Tyson PD, Mason SJ (1997) Mesoscale modelling of tropical-temperature troughs and associated systems over southern Africa. WRC Report 595/1/97, 395 pp

Engelbrecht CJ, Engelbrecht FA, Dyson LL (2013) High-resolution model-projected changes in mid-tropospheric closed-lows and extreme rainfall events over southern Africa. International Journal of Climatology 33:173-187 DOI: 10.1002/joc.3420

Fauchereau N, Pohl B, Reason CJC, Rouault M, Richard Y (2009) Recurrent daily OLR patterns in the Southern Africa/Southwest Indian Ocean region, implications for South African rainfall and teleconnections. Climate Dynamics 32: 575-591 DOI: 10.1007/s00382-008-0426-2

Favre A, Hewitson B, Lennard C, Cerezo-Mota R, Tadross M (2012) Cut-off lows in the South Africa region and their contribution to precipitation. Climate Dynamics. DOI: 10.1007/s00382-012-1579-6

Harris I, Jones, PD, Osborn TJ, Lister DH (2013) Updated high-resolution grids of monthly climatic observations – the CRU TS3.10 dataset. International Journal of Climatology. DOI: 10.1002/joc.3711

Hart NCT, Reason CJC, Fauchereau N (2012) Cloud bands over southern Africa: seasonality, contribution to rainfall variability and modulation by the MJO. Climate Dynamics. DOI: 10.1007/s00382-012-1589-4

Hayward LQ, van den Berg H (1968) Die Port Elizabeth-stortreens van 1 September 1968. SA Weather Bureau News Letter No. 234, 157-169

Hayward LQ, van den Berg H (1970) The Eastern Cape Floods of 24 to 28 August, 1970. SA Weather Bureau News Letter No. 257, 129-141

Hewitson BC, Crane RG (2002) Self-organizing maps: Applications to synoptic climatology. Climate Research 22: 13-26

Jury MR, Levey K (1993) The climatology and characteristics of drought in the eastern Cape of South Africa. International Journal of Climatology 13: 629-641. DOI: 10.1002/joc.3370130604

686 Kalnay E, Kanamitsu M, Kistler R, Collins W, Deaven D, Gandin L, Iredell M, Saha S, White G,
687 Woollen J, Zhu Y, Leetmaa A, Reynolds B, Chelliah M, Ebisuzaki W, Higgins W, Janowiak J,
688 Mo KC, Ropelewski C, Wang J, Jenne R, Joseph D (1996) The NCEP/NCAR 40-year reanalysis
689 project. Bulletin of the American Meteorological Society 77: 437-471
690
691 Katzfey JJ, McInnes KL (1996) GCM simulations of Eastern Australia cutoff lows. Journal of Climate
692 9: 2337-2355
693
694 Kohonen T (2001) Self-Organizing Maps. 3rd ed. Springer, 501 pp
695
696 Landman WA, Mason SJ, Tyson PD, Tennant WJ (2001) Retro-active skill of multi-tiered forecasts of
697 summer rainfall over southern Africa. International Journal of Climatology 21: 1-19
698
699 Malherbe J, Engelbrecht FA, Landman WA, Engelbrecht CJ (2012) Tropical systems from the
700 southwest Indian Ocean making landfall over the Limpopo River Basin, southern Africa: a historical
701 perspective. International Journal of Climatology 32: 1018-1032 DOI: 10.1002/joc.2320
702
703 Muller A, Reason CJC, Fauchereau N (2008) Extreme rainfall in the Namib Desert during late summer
704 2006 and influences of regional ocean variability. International Journal of Climatology 28: 1061-1070.
705 DOI: 10.1002/joc.1603
706
707 Philippon N, Rouault M, Richard Y, Favre A (2011) The influence of ENSO on winter rainfall in South
708 Africa. International Journal of Climatology 32: 2333-2347. DOI: 10.1002/joc.3403.
709
710 Roberts CPR, Alexander WJR (1982) Lessons learnt from the 1981 Laingsburg flood. Civil Engineer
711 in South Africa 24: 17-21, 24-25, 27
712
713 Rouault M, White SA, Reason CJC, Lutjehams JRE, Jobard I (2002) Ocean-Atmosphere interaction in
714 the Agulhas current region and a South African extreme Weather event. Weather and Forecasting 17:
715 655-669
716
717 Rouault M, Richard Y (2003) Intensity and spatial extension of drought in South Africa at different
718 time scales. Water SA 29: 489-500
719
720 Schuenemann KC, Cassano JJ, Finnis J (2009) Synoptic Forcing of Precipitation over Greenland:
721 Climatoloy for 1961-99. Journal of Hydrometeorology 10: 60-78
722
723 Singleton AT, Reason CJ (2006) A numerical model study of an intense cutoff low pressure system
724 over South Africa. Monthly Weather Review 135: 1128-1150
725
726 Singleton AT, Reason CJ (2007a) Numerical simulations of a severe rainfall event over the Eastern
727 Cape coast of South Africa: sensitivity to sea surface temperature and topography. Tellus 58: 355-367
728
729 Singleton AT, Reason CJ (2007b) Variability in the characteristics of cut-off low pressure systems over
730 subtropical southern Africa. International Journal of Climatology 27: 295-310
731
732 Sylla MB, Giorgi F, Coppola E, Mariotti L (2012) Uncertainties in daily rainfall over Africa:
733 assessment of gridded observation products and evaluation of a regional climate model simulation.
734 International Journal of Climatology. DOI: 10.1002/joc.3551
735
736 Taljaard JJ (1985) Cut-off lows in the South African region. South African Weather Bureau, technical
737 paper 14
738
739 Taljaard JJ (1995) Atmospheric circulation systems, synoptic climatology and weather phenomena of
740 South Africa. Part 2: Atmospheric circulation systems in the South African region. South African
741 Weather Bureau, technical paper 28
742
743 Taljaard JJ (1996) Atmospheric circulation systems, synoptic climatology and weather phenomena of
744 South Africa. Part 6: Rainfall in South Africa. South African Weather Bureau, technical paper 32
745

746 Tennant WJ (2003) An assessment of intraseasonal variability from 13-yr GCM Simulations. Monthly
747 Weather Review 131: 1975-1991
748
749 Tennant WJ (2004) Considerations when using pre-1979 NCEP/NCAR reanalysis in the southern
750 hemisphere. Geophysical Research Letters 31: L11112. DOI: 10/1029/2004GLO197501
751
752 Tennant WJ, van Heerden J (1994) The influence of orography and local sea-surface temperature
753 anomalies on the development of the 1987 Natal floods: a general circulation model study. Suid-
754 Afrikaanse Tydskrif vir Wetenskap 90: 45-49
755
756 Tennant WJ, Hewitson BC (2002) Intra-seasonal rainfall characteristics and their importance to the
757 seasonal prediction problem. International Journal of Climatology 22: 1033-1048. DOI:
758 10.1002/joc.778
759
760 Tozuka T, Abiodun BJ, Engelbrecht FA (2013) Impacts of convection schemes on simulating tropical-
761 temperate troughs over southern Africa. Climate Dynamics. DOI: 10.1007/s00382-013-1738-4
762
763 Van Rooy MP (1972) Climate of South Africa: District rainfall for South Africa and the annual march
764 of rainfall over southern Africa, part 10. South African Weather Bureau Tech. Note WB 35, Dept. of
765 Transport, Pretoria, South Africa, 116 pp.
766
767 Van Schalkwyk L, Dyson LL (2013) Climatological characteristics of fog at Cape Town International
768 airport. Weather and Forecasting. DOI: 10.1175/WAF-D-12-00028.1
769
770 Weldon D, Reason CJC (2013) Variability of rainfall characteristics over the South Coast region of
771 South Africa. Theoretical and Applied Climatology. DOI: 10.1007/s00704-013-0882-4

Figure

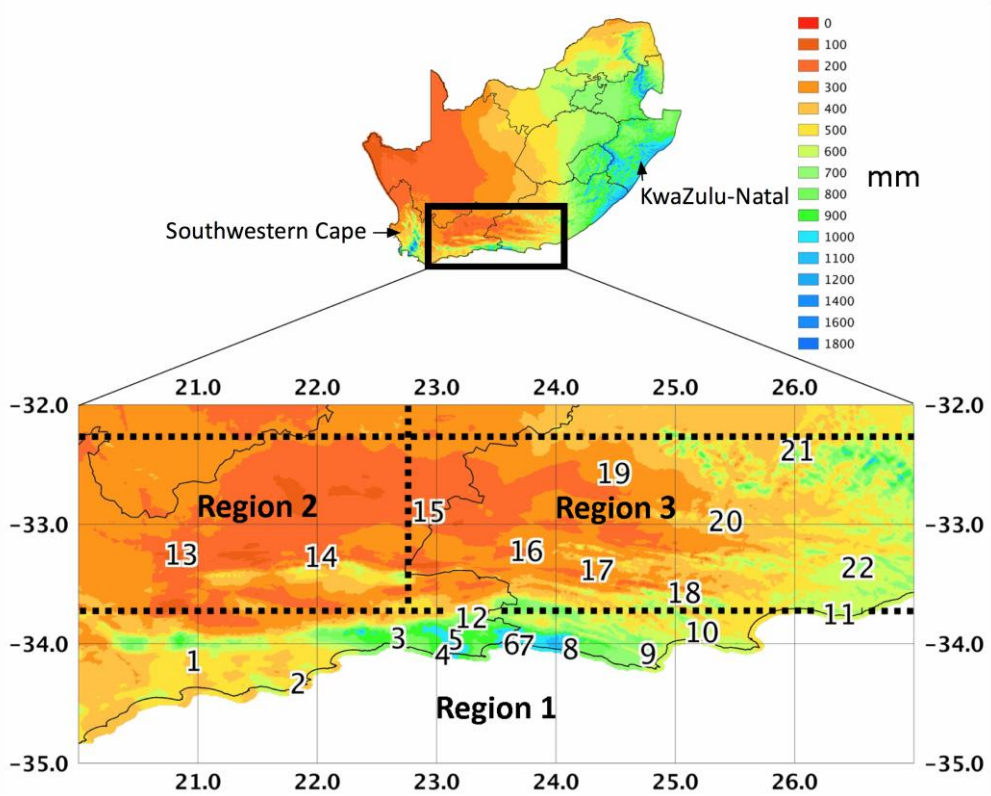

Fig. 1 The geographic location of the study region within South Africa (indicated by the rectangle - solid black lines). The 3 sub-regions of interest, labeled as Region 1, Region 2 and Region 3, are delineated by the black dotted lines on the zoomed-in view of the study region. Numbers 1 to 21 indicate the selected rainfall stations used in the analysis of rainfall attributes. The background shaded colour contours of the mean annual rainfall are based on the ARC in-house developed gridded rainfall dataset

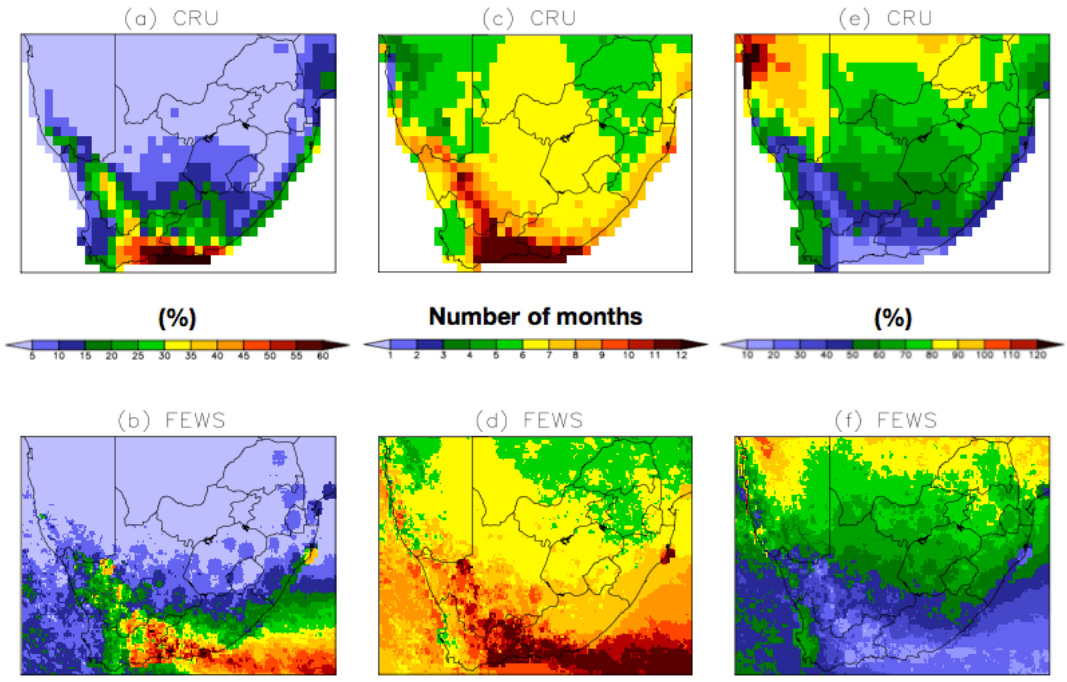

Fig. 2 Delineation of rainfall regions in South Africa according to the ratio of the month of minimum rainfall to the month of maximum rainfall (a, b), the number of months for which the mean monthly rainfall total contributes 5% or more to the mean annual rainfall total (c, d), and the average fluctuation of monthly rainfall from the monthly main rainfall expressed as a percentage (e, f), calculated from CRU (a, c, e) and FEWS (b, d, f) data for the period 1983-2009

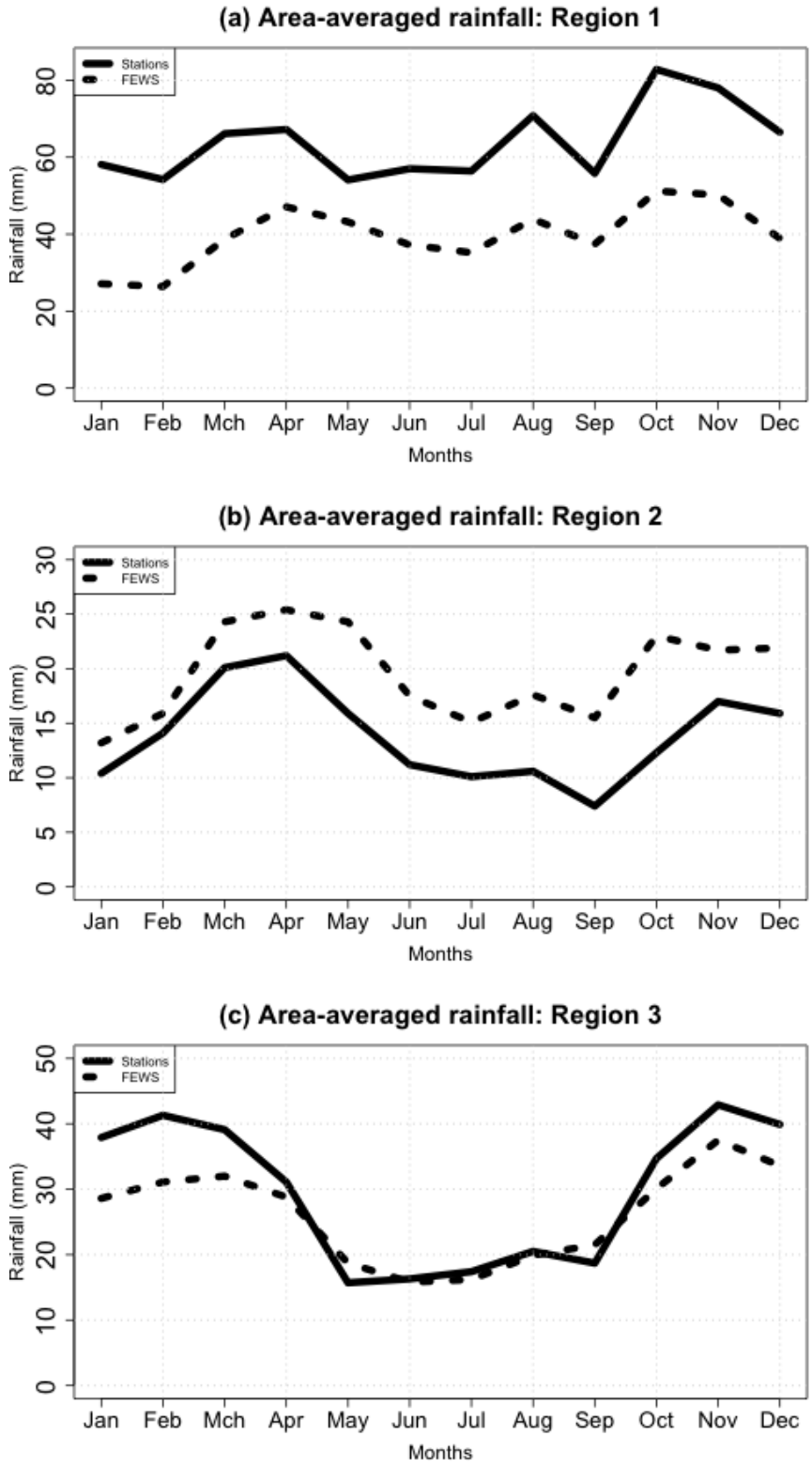

Fig. 3 Area-averaged annual rainfall cycle for the period 1979-2011 over (a) Region 1, (b) Region 2 and (c) Region 3 as described by weather station data (solid line) and FEWS rainfall (dotted line)

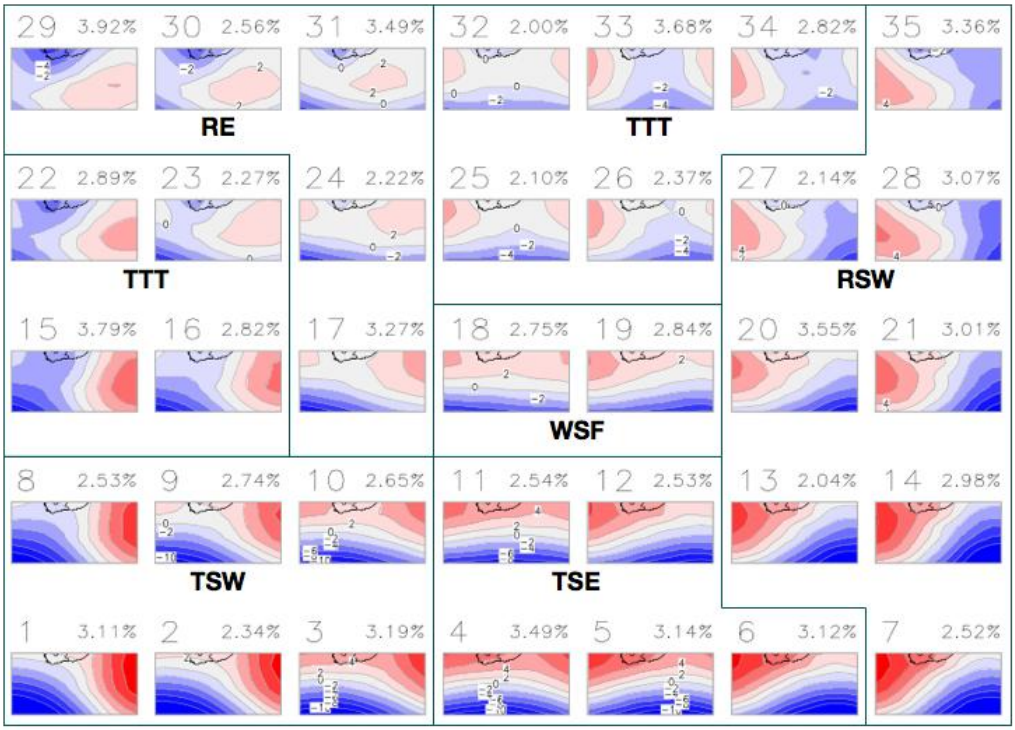

Fig. 4 SOM of SLP anomalies (hPa) based on daily NCEP reanalysis data from 1979 to 2011. Anomaly SLP contour interval is 2 hPa. Blue and red shades represent negative and positive SLP anomalies, respectively. The node numbers as well as the node frequency of occurrence are indicated on the figure. Nodes occurring outside the range of 2.56-3.15%, have lower or higher than average occurrences statistical significant at the 95% confidence level. Subjective clustering of the main synoptic types is indicated and represent ridging high pressure systems southeast of the subcontinent (RE), tropical-temperate troughs (TTT), troughs southwest of the subcontinent (TSW), troughs southeast of the subcontinent (TSE), ridging high pressure systems from the southwest (RSW) and weak synoptic flow (WSF)

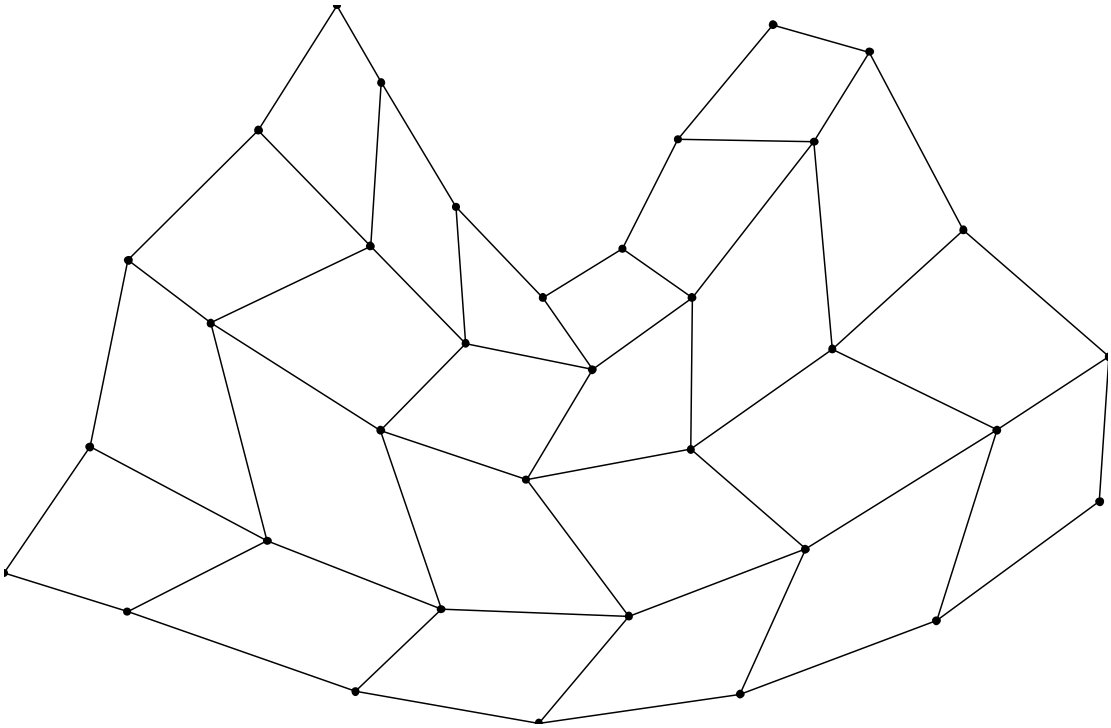

Fig. 5 Sammon map for the SOM shown in Fig. 4

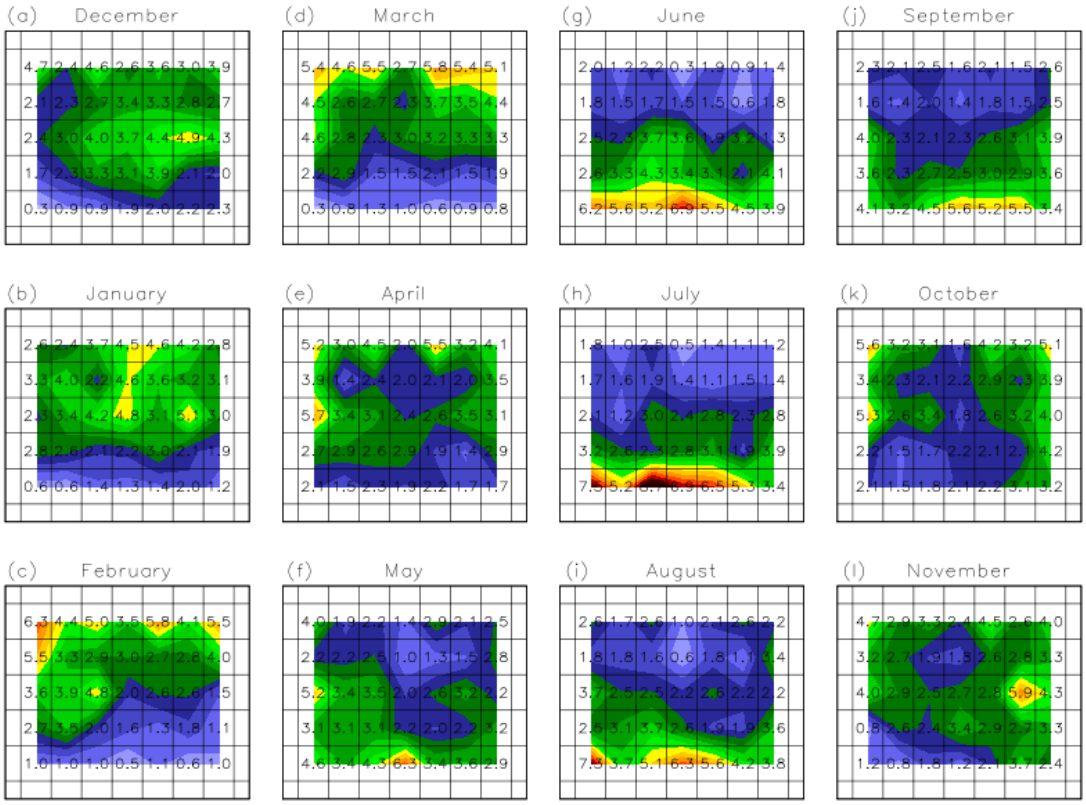

Fig. 6 Node frequencies (%) for (a) December (1023 days), (b) January (1023 days), (c) February (932 days), (d) March (1023 days), (e) April (990 days), (f) May (1023 days), (g) June (990 days), (h) July (1023 days), (i) August (1023 days), (j) September (990 days), (k) October (1023 days) and (l) November (990 days) that map to each node based on the total days of the particular month from 1979-2011

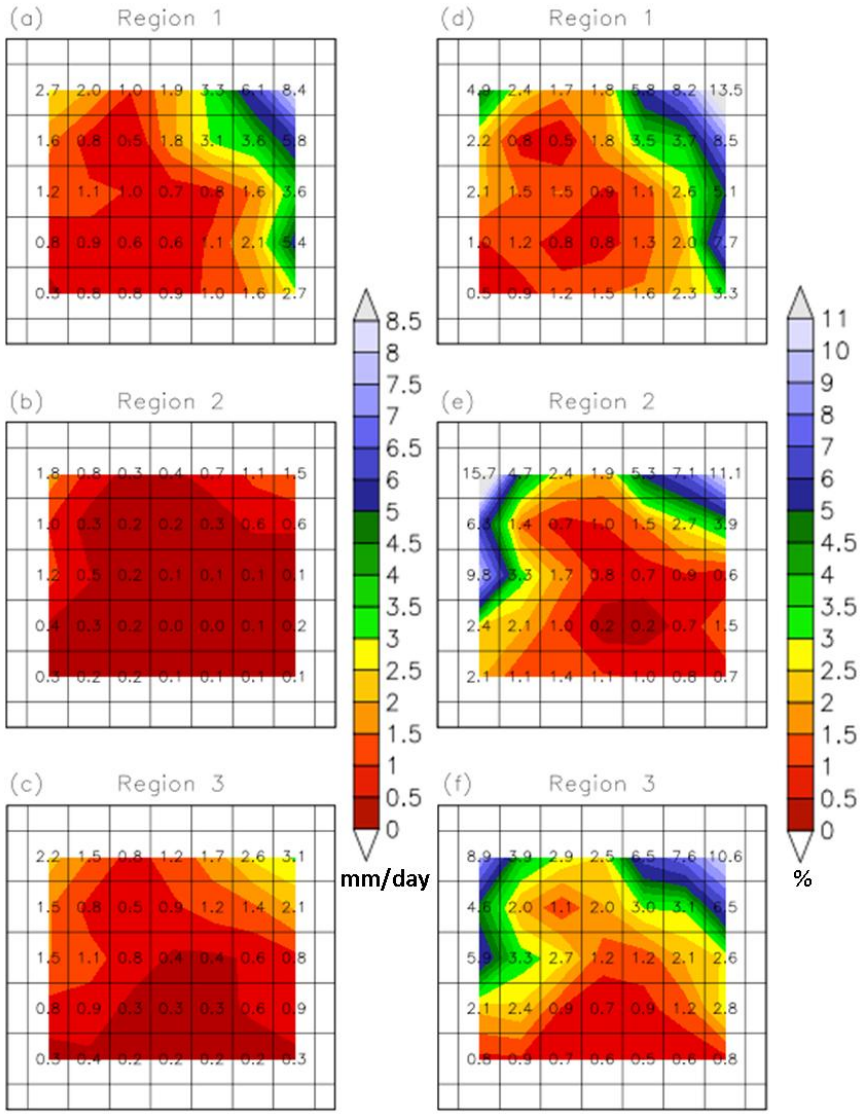

Fig. 7 The regionally averaged daily precipitation (mm/day) for each SOM node for (a) Region 1, (b) Region 2 and (c) Region 3, and the average annual contribution (%) by node to rainfall over (d) Region 1, (e) Region 2 and (f) Region 3

Fig. 8 Accumulated frequency of rainfall-producing COLs (units: COL days/grid point) for each SOM node for the period 1979-2011. Only grid points with a frequency of at least 1 day are indicated

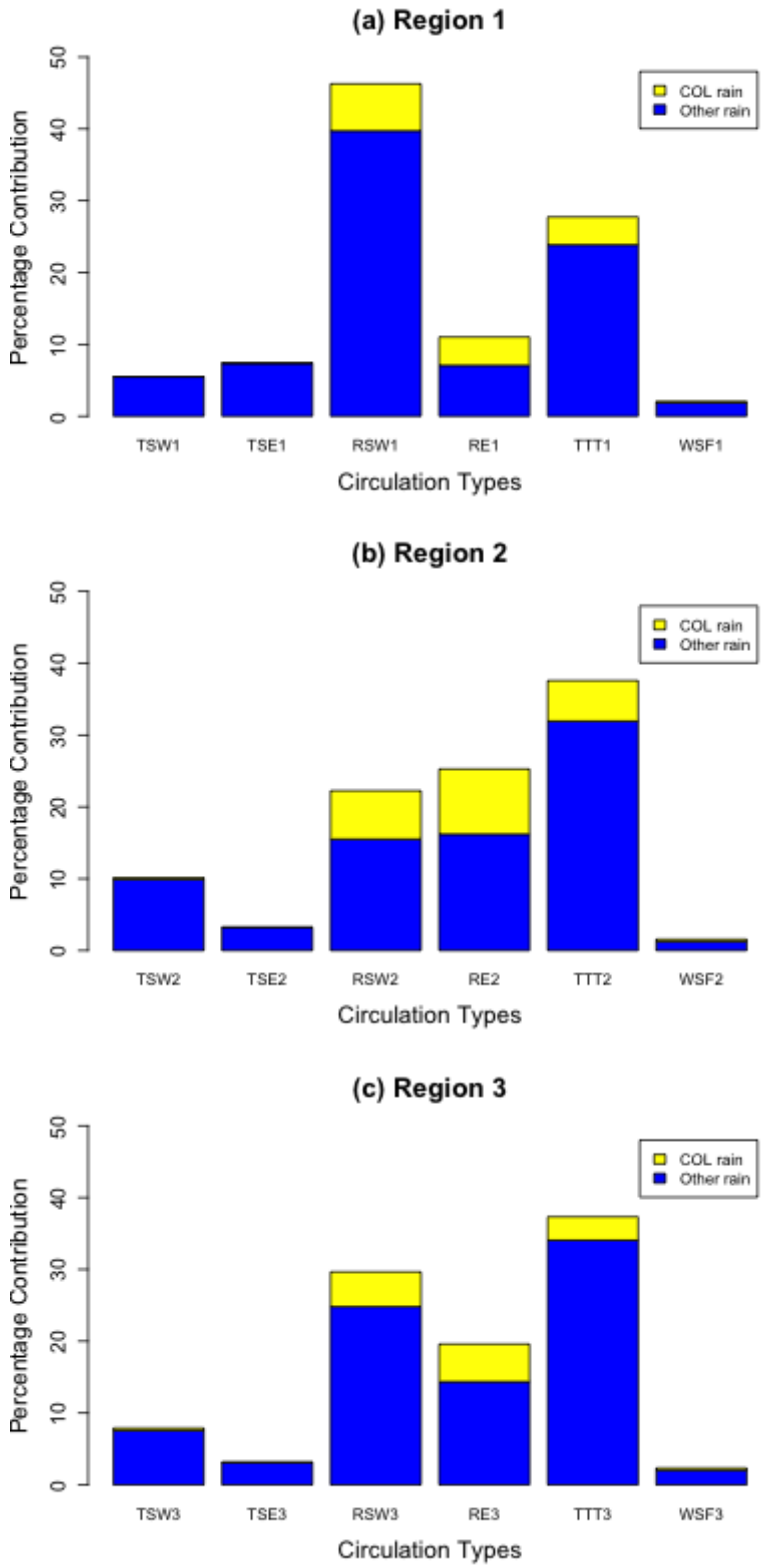

Fig. 9 The percentage contribution to the average annual rainfall of the 6 main synoptic classes identified in this study for (a) Region 1, (b) Region 2 and (c) Region 3. The percentage of rainfall contributed by COLs to the average rainfall, in association with the six main synoptic classes, is shown in yellow

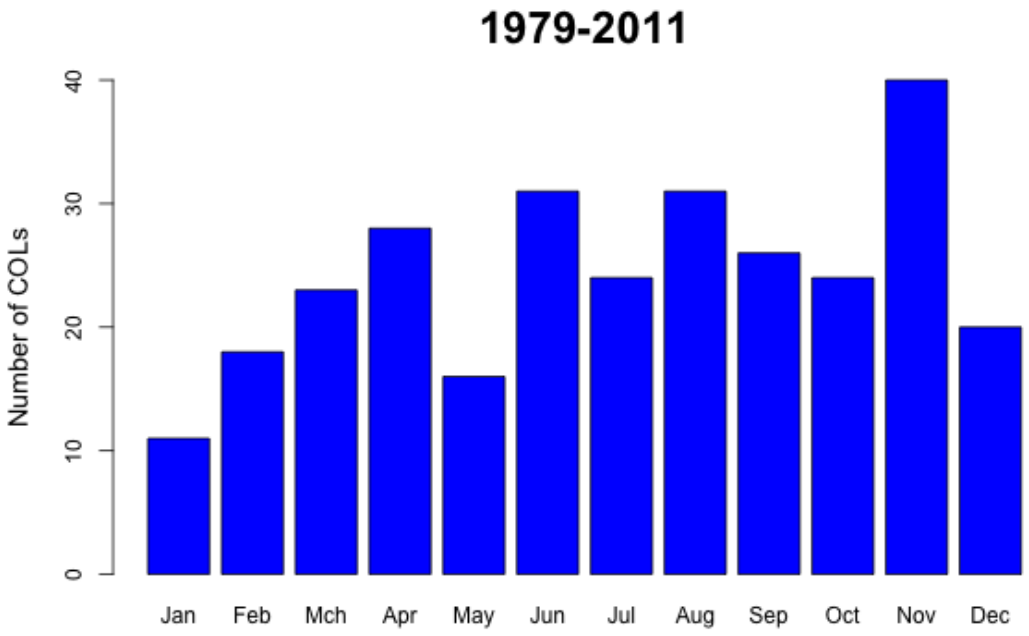

Fig. 10 Accumulated monthly number of COLs within 1100 km from the centroid of the study region and associated with rainfall at 1 station or more, over the period 1979-2011

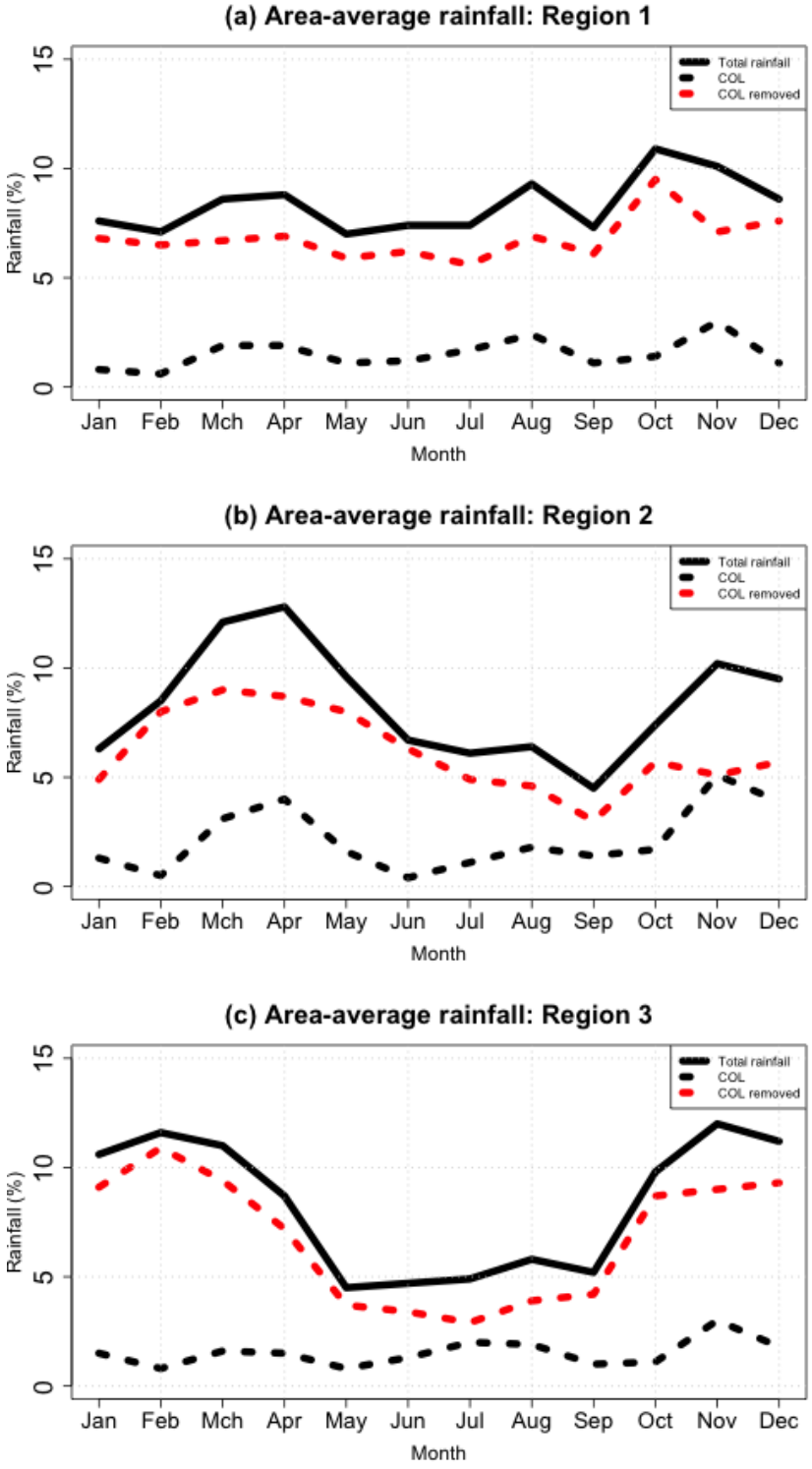

Fig. 11 Area-average annual rainfall distribution for the period 1979-2011 over (a) Region 1, (b) Region 2 and (c) Region 3. The black solid line represents the monthly rainfall (%), the black dotted line the monthly rainfall associated with COLs (%) and the red dotted line the monthly rainfall without the COL-induced rainfall (%)

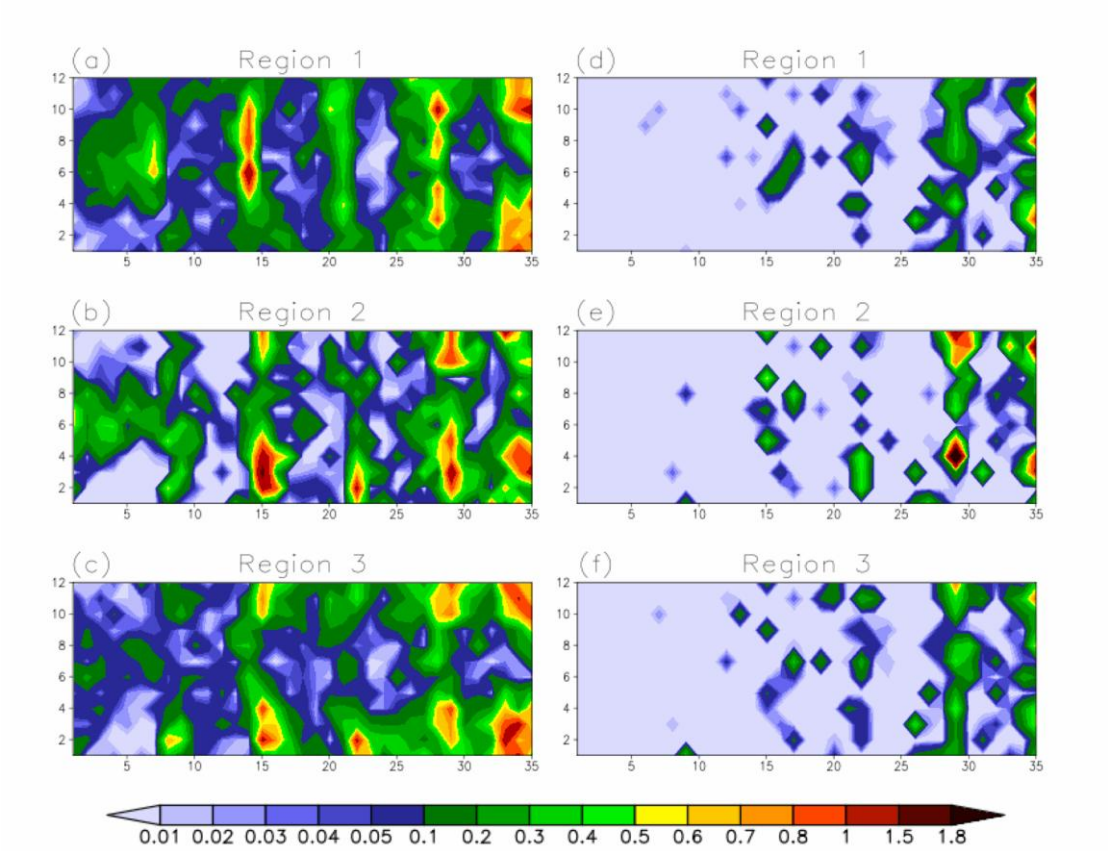

Fig. 12 Percentage contributions of monthly rainfall totals to the average annual rainfall (y-axis) not associated with COLs for (a) Region 1, (b) Region 2, (c) Region 3 and associated with COLs for (d) Region 1, (e) Region 2 and (f) Region 3. The 35 SOM nodes are indicated on the x-axis

Fig1

Click here to download high resolution image

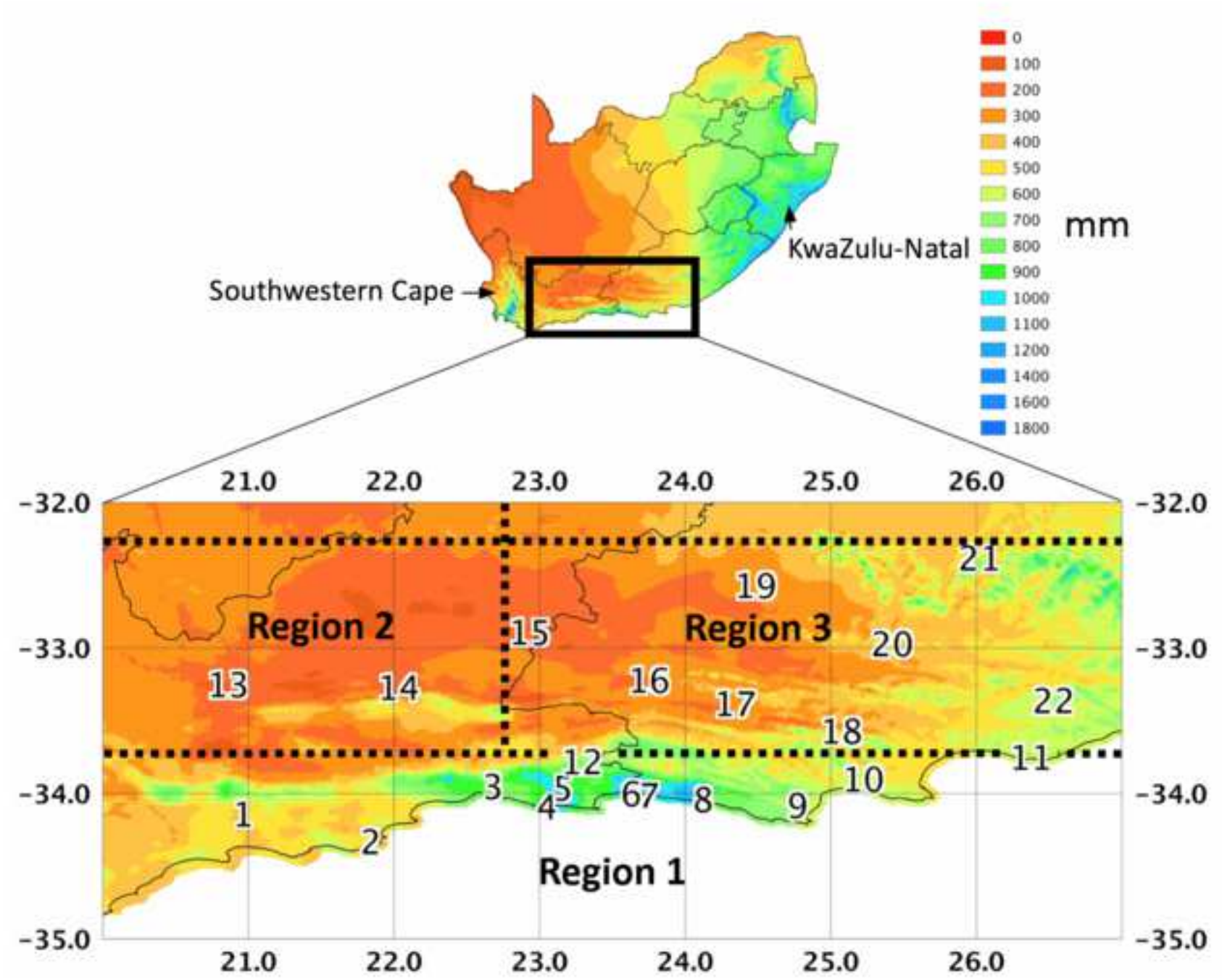

Fig2
Click here to download high resolution image

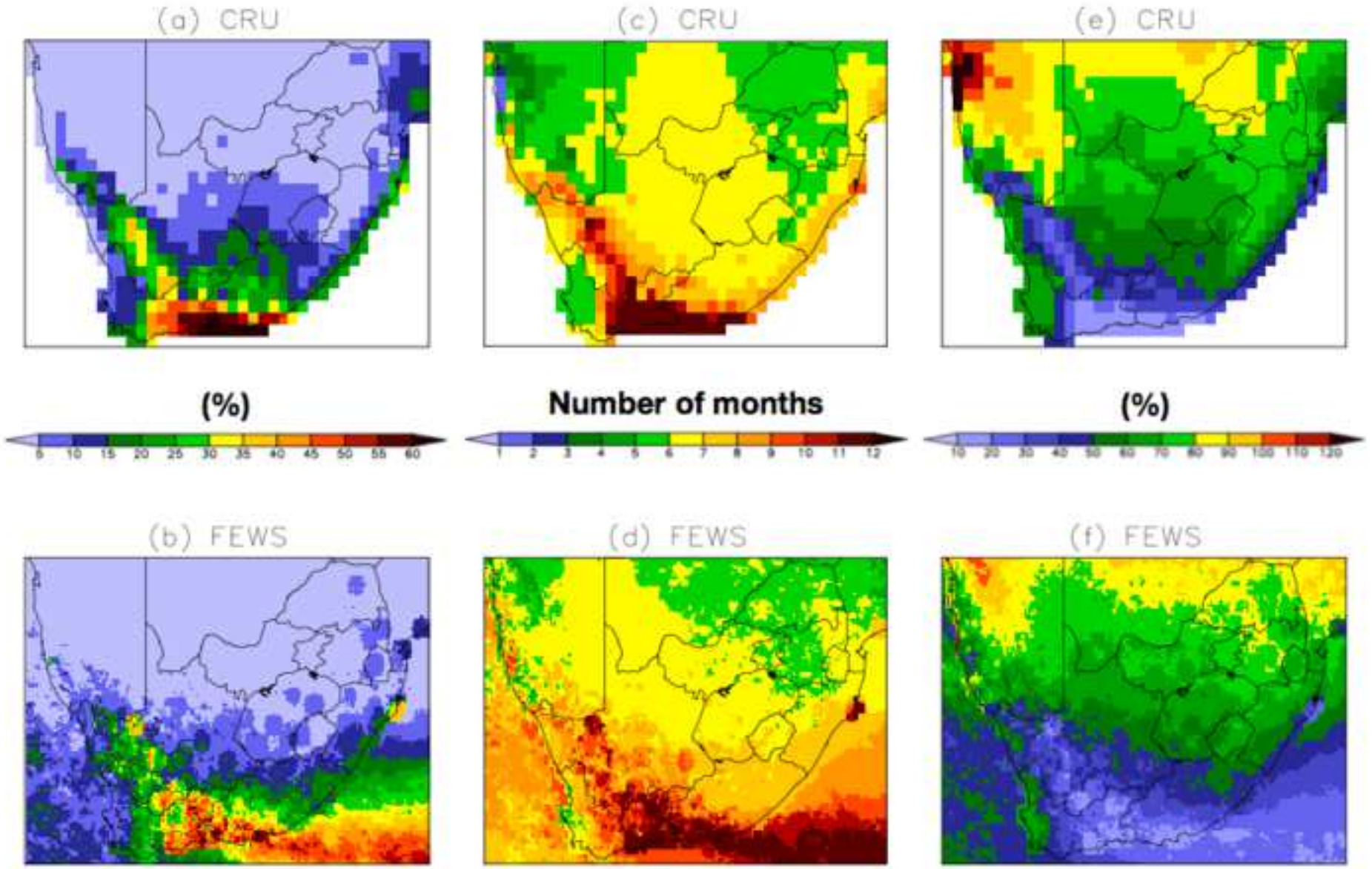

Fig3
Click here to download high resolution image

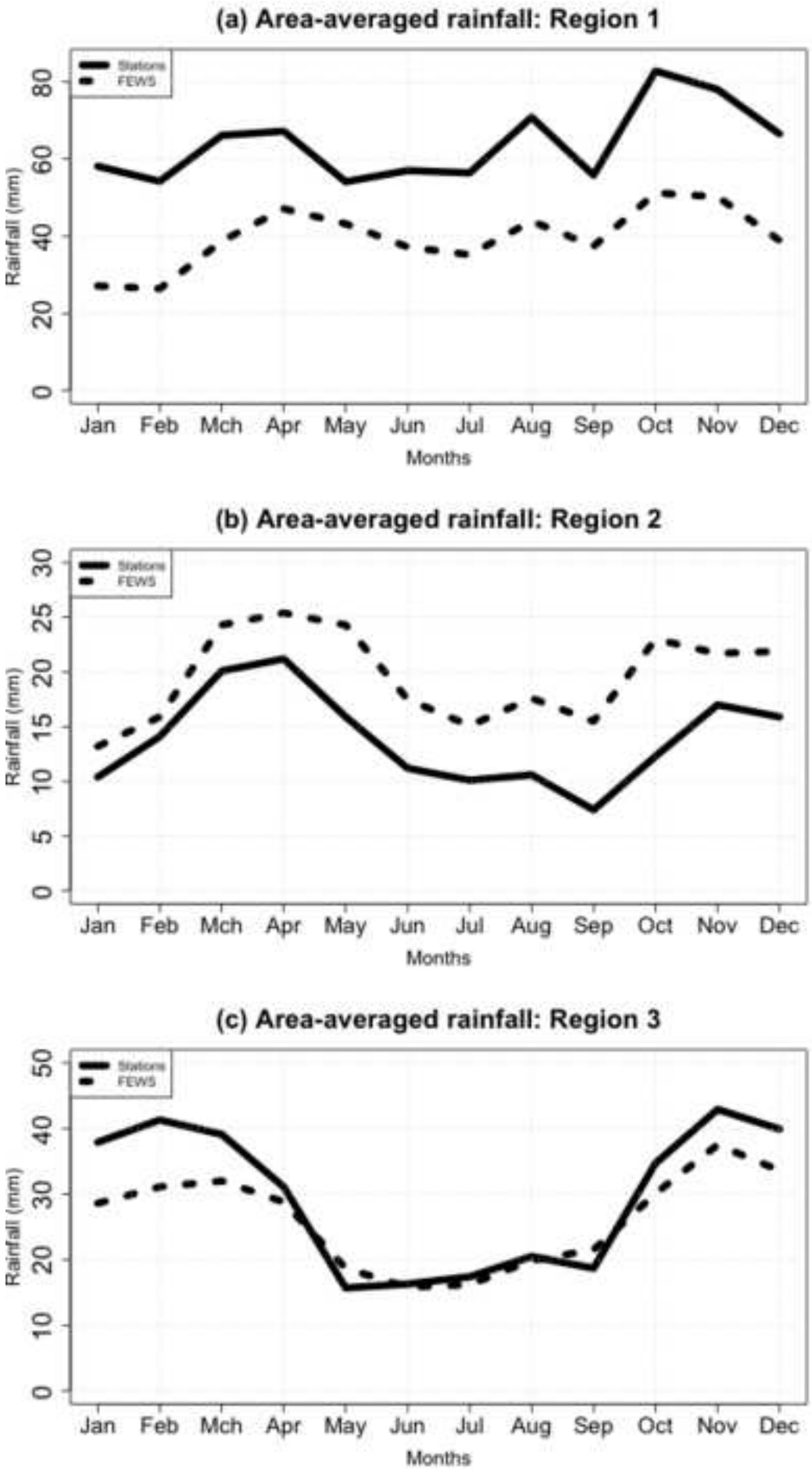

Fig4

Click here to download high resolution image

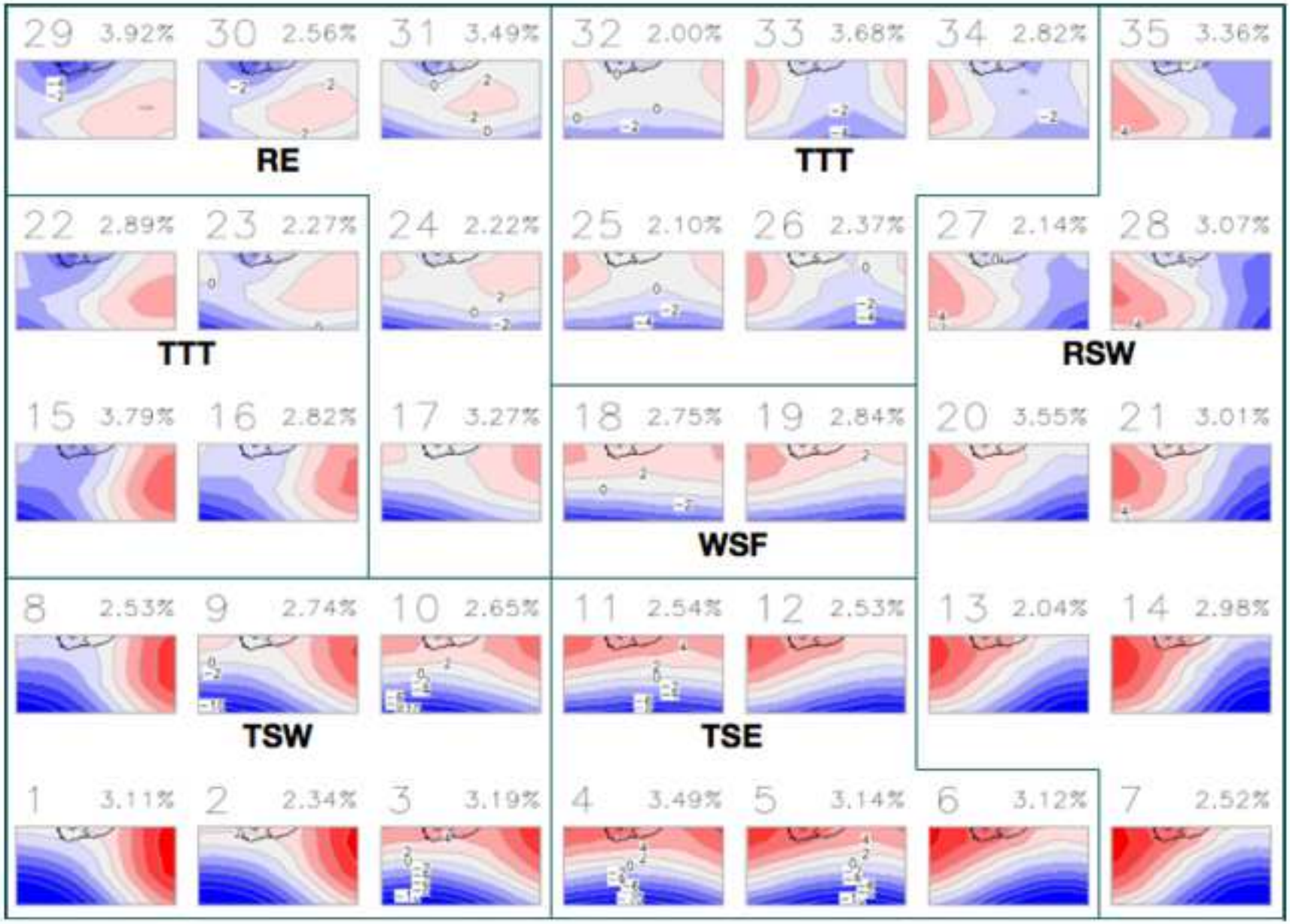

Fig5

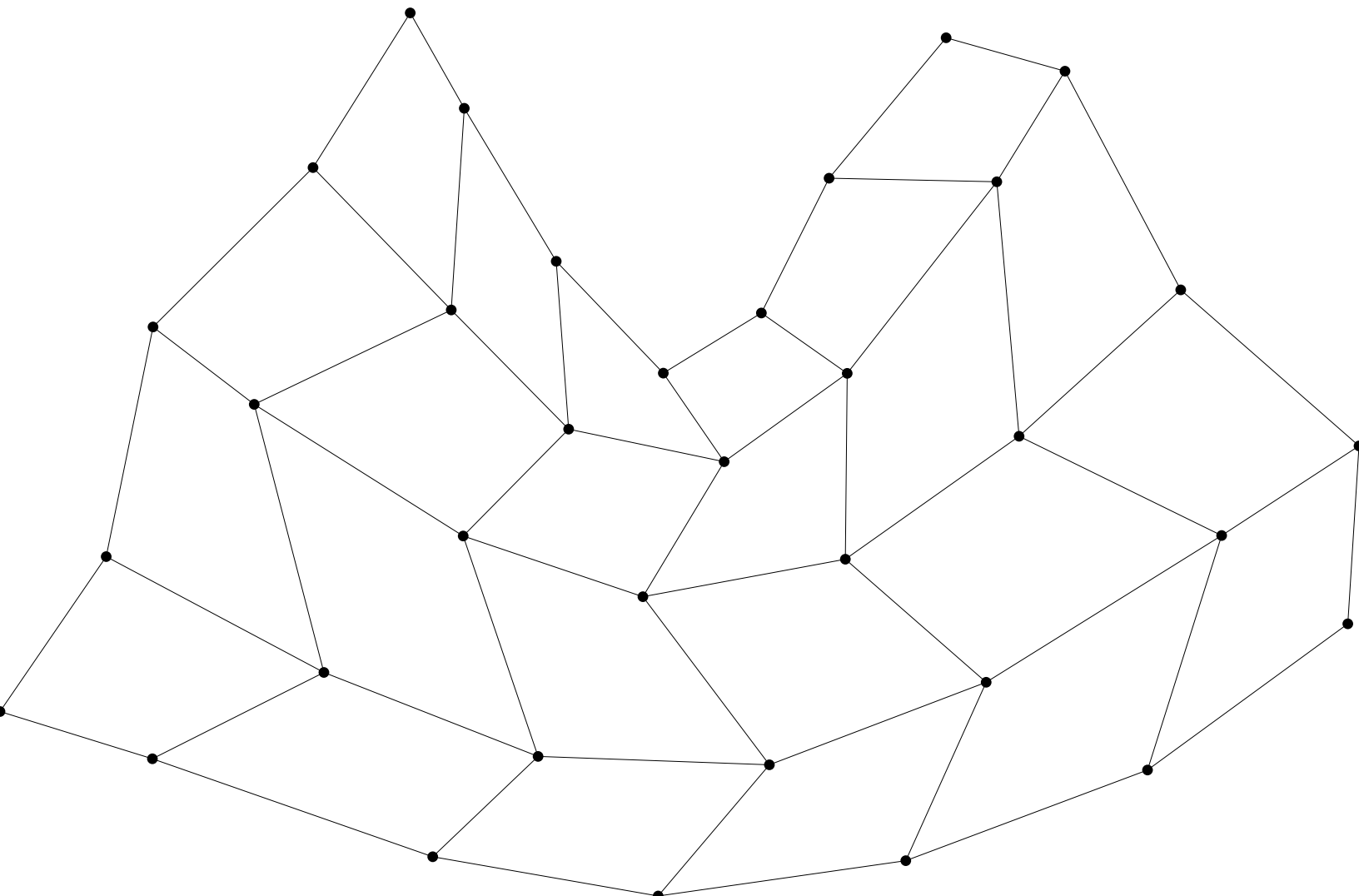

Fig6

Click here to download high resolution image

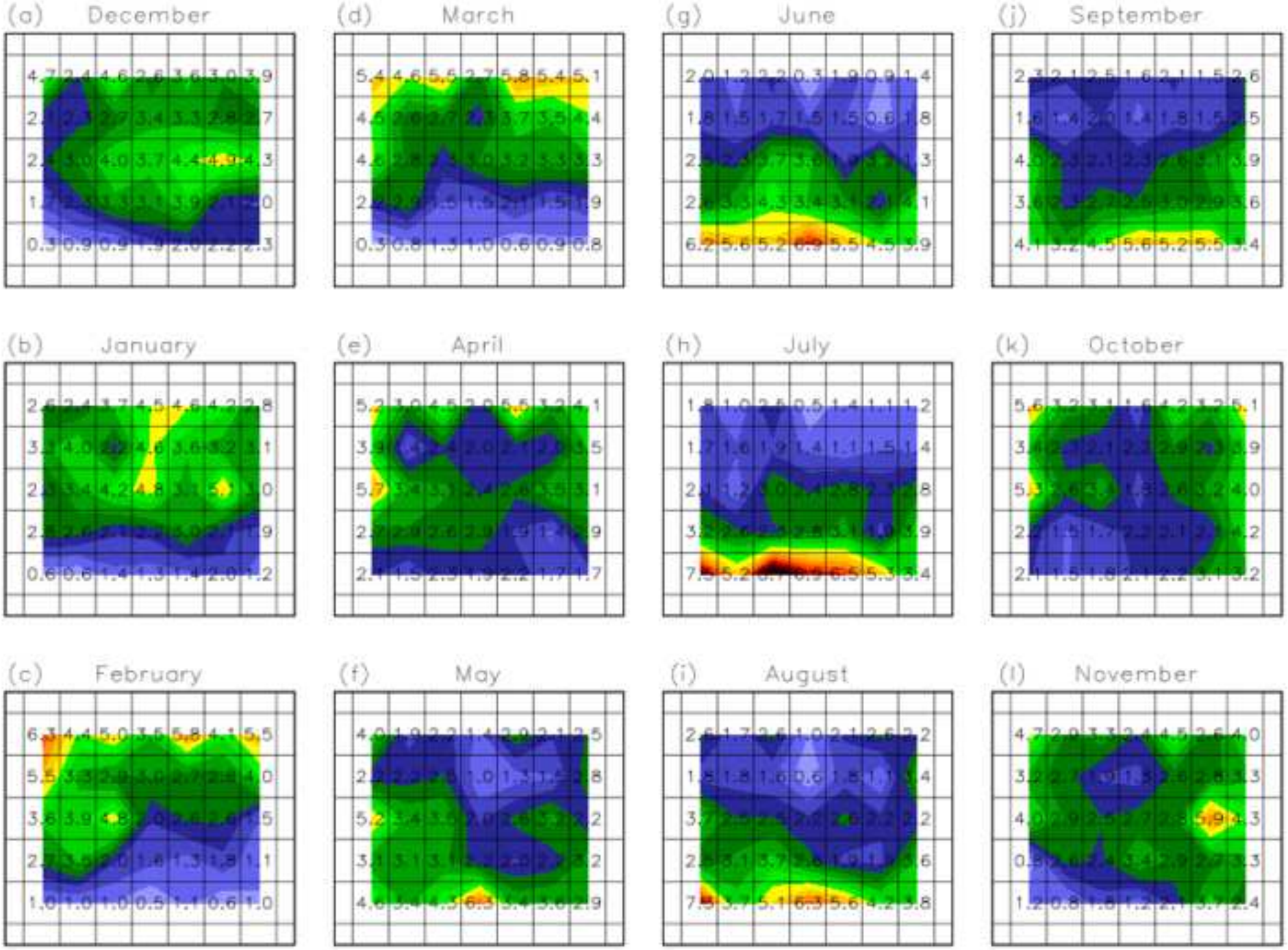

Fig7

Click here to download high resolution image

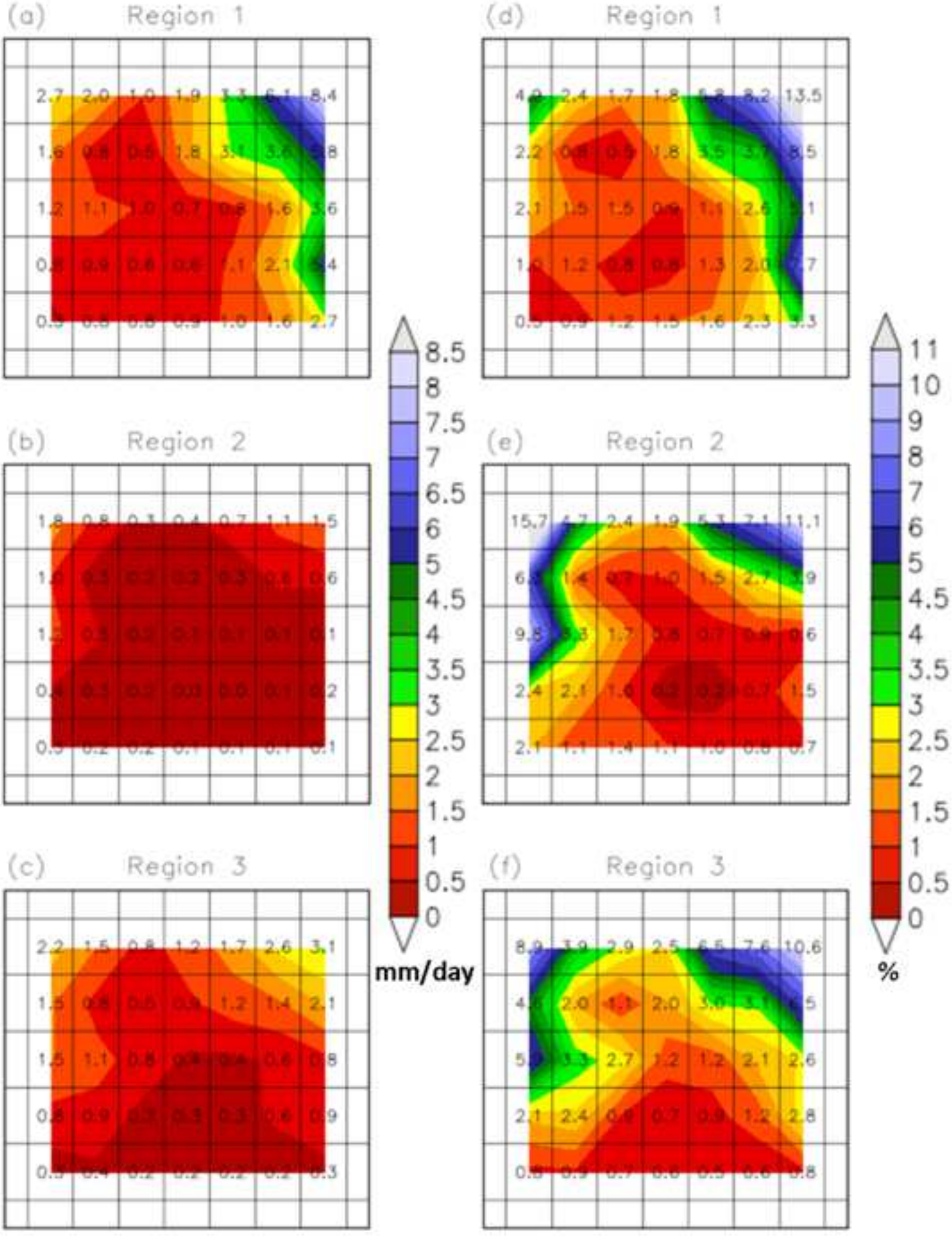

Fig8

Click here to download high resolution image

Fig9
Click here to download high resolution image

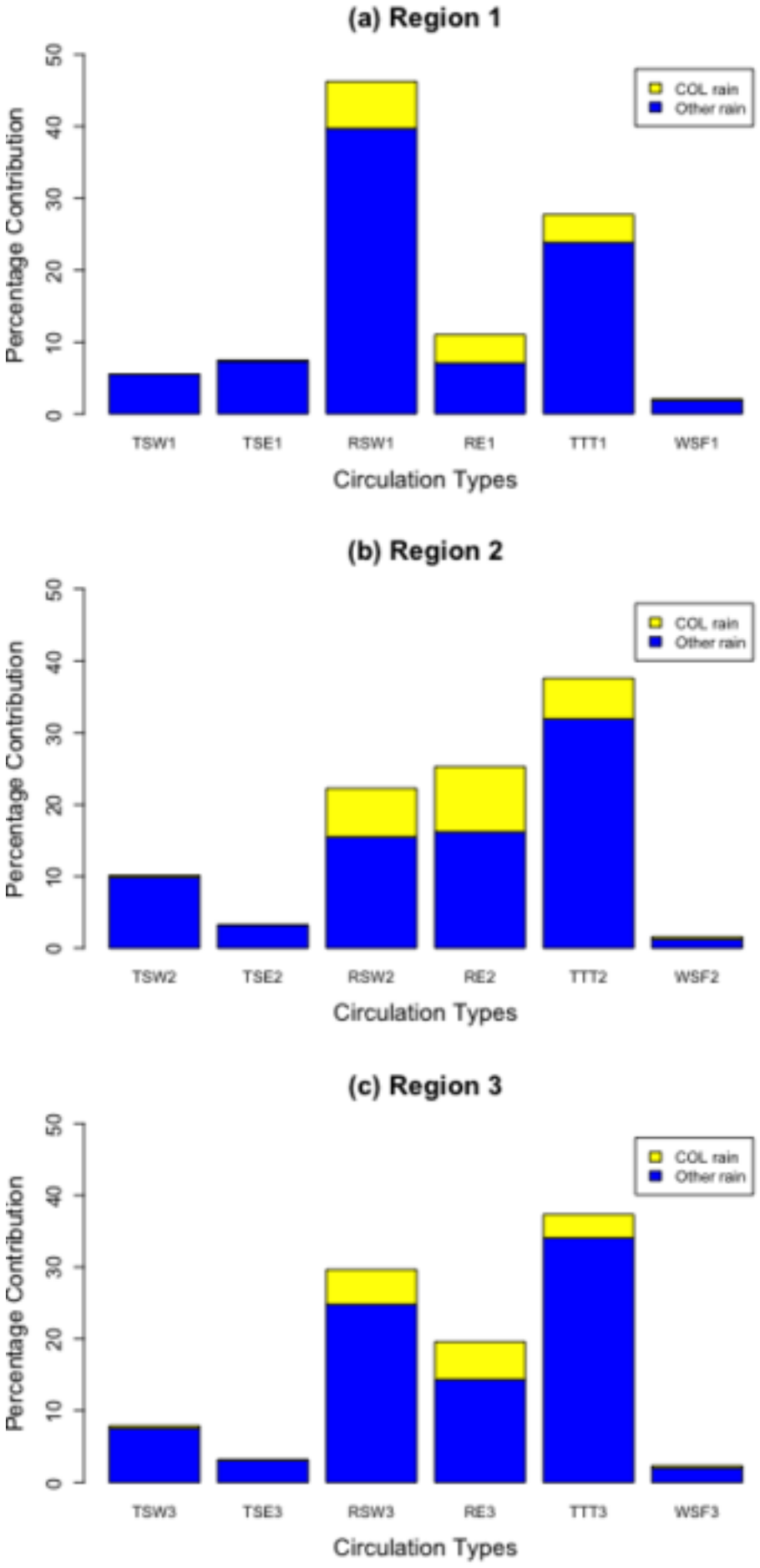

Fig10
Click here to download high resolution image

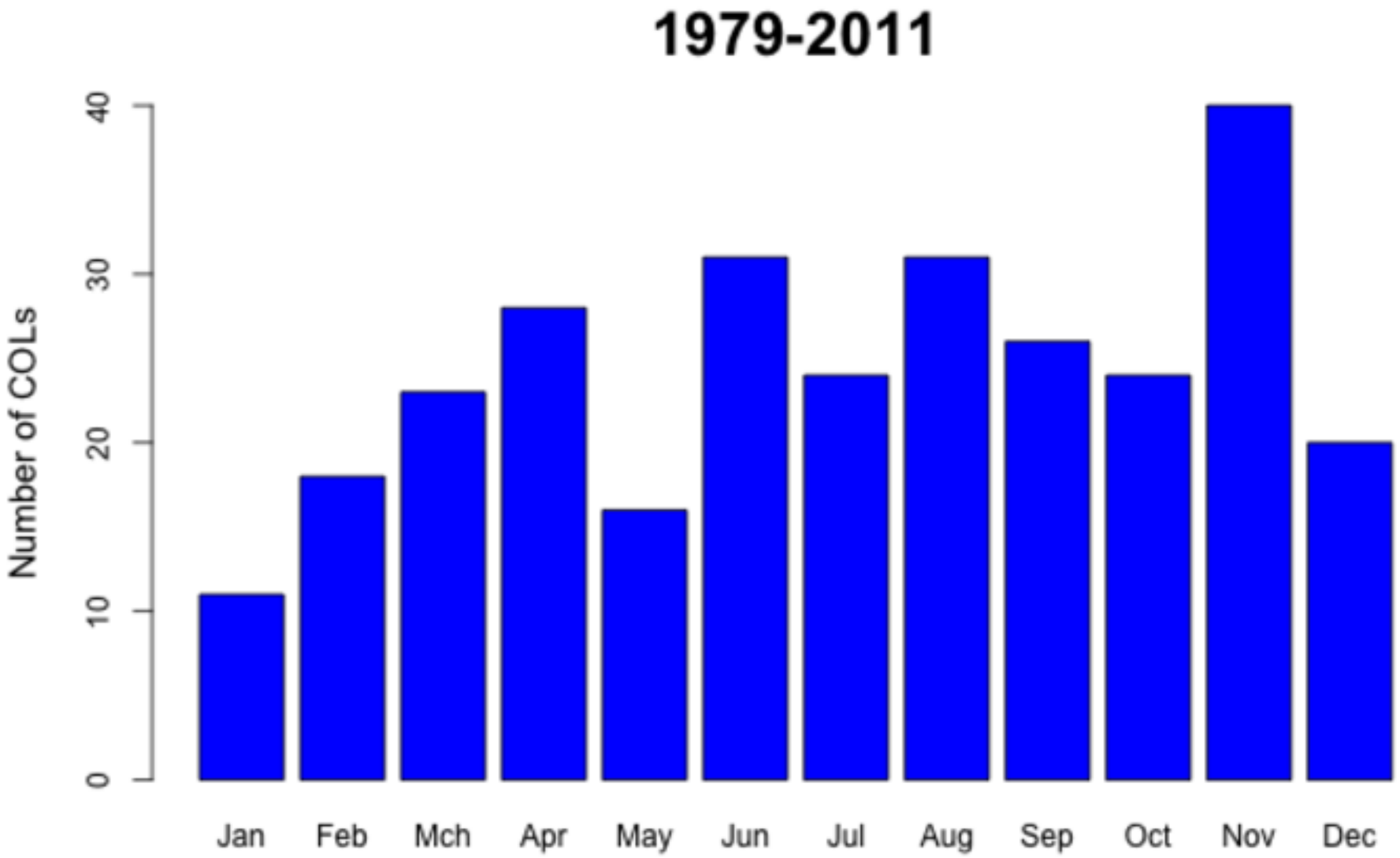

Fig11
Click here to download high resolution image

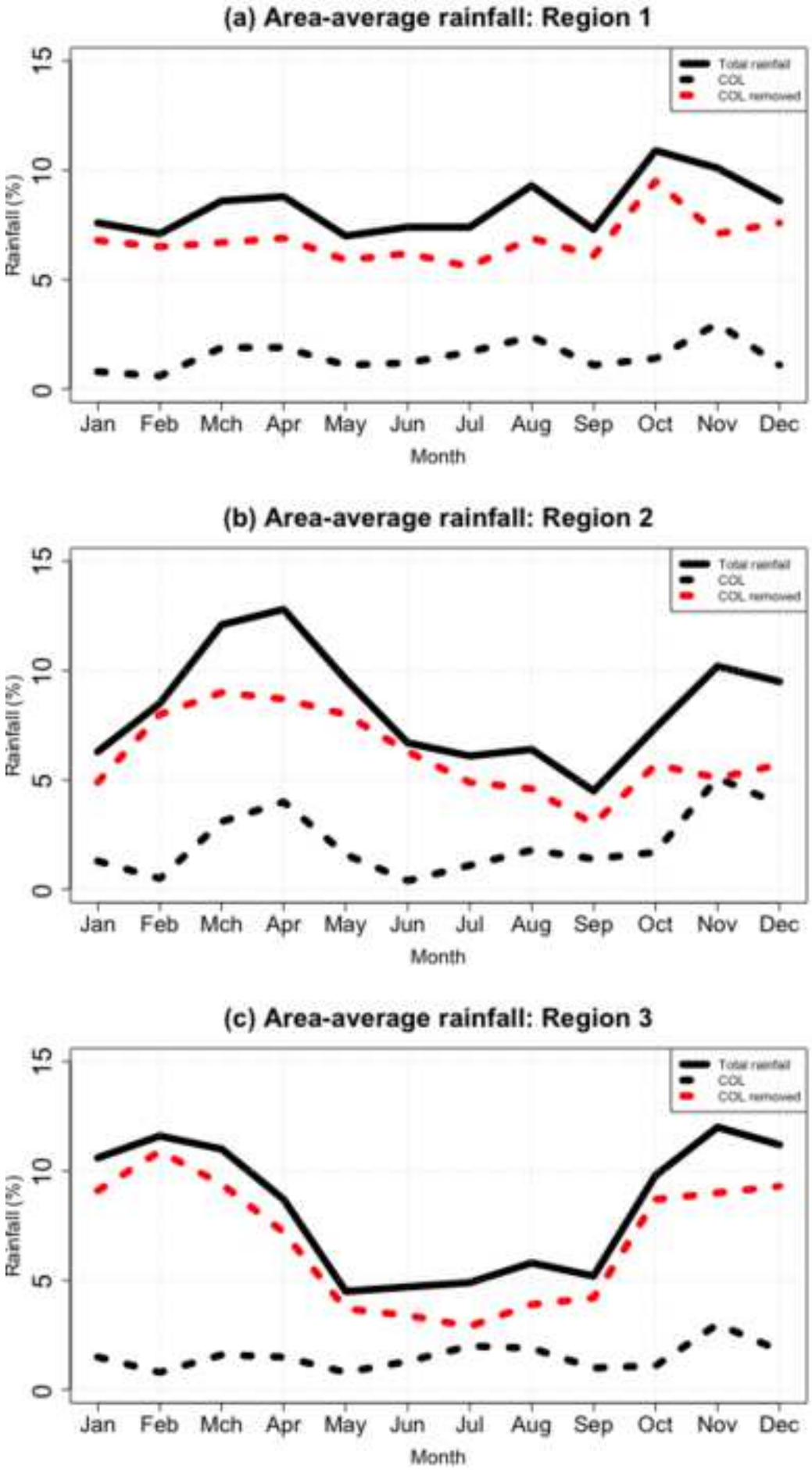

Fig12

Click here to download high resolution image